Bloch-Optimized Dithered-Ultrasound-Pulse RF for Low-Field Inhomogeneous Permanent Magnet MR Imagers

Irene Kuang[1], Nicolas Arango[1], Jason Stockmann[2,3], Elfar Adalsteinsson[1,4], Jacob White[1]

[1]Department of Electrical Engineering and Computer Science, Massachusetts Institute of Technology, Cambridge, MA, United States,
[2]Athinoula A. Martinos Center for Biomedical Imaging, Massachusetts General Hospital, Charlestown, MA, United States,
[3]Harvard Medical School, Boston, MA, United States,
[4]Institute for Medical Engineering and Science, Massachusetts Institute of Technology, Cambridge, MA, United States

Massachusetts Institute of Technology

MGH/HST Athinoula A. Martinos Center for Biomedical Imaging

Massachusetts General Hospital

Harvard-MIT Health Sciences & Technology

Harvard Medical School

Declaration of Financial Interests or Relationships

Speaker Name: Irene Kuang

I have no financial interests or relationships to disclose with regard to the subject matter of this presentation.

Permanent Magnet MR Imagers

✓Low cost

✓Portable

✓Safe for point-of-care and classroom use

—Inhomogeneous compared to clinical scanners (<1 ppm over head)

—Large negative temperature coefficient (thousands of ppm/ °C)

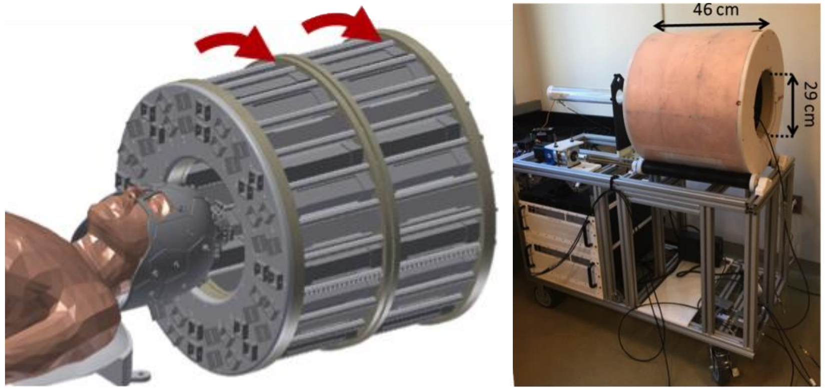

20,000 ppm

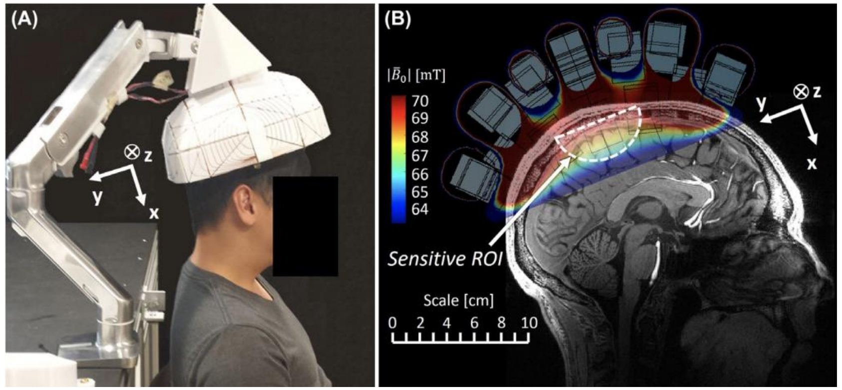

10,000 ppm

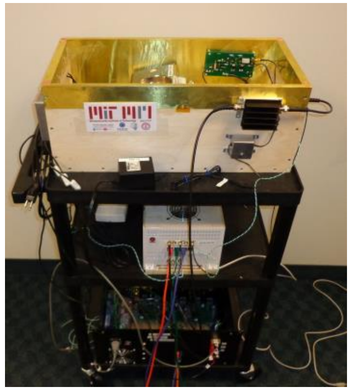

50 ppm

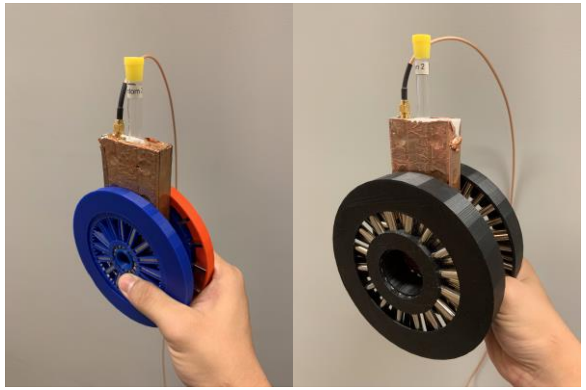

500-5,000 ppm

[1] Cooley et al., *Design of sparse Halbach magnet arrays for portable MRI using a genetic algorithm*. IEEE Trans. Magn., 2018.
[2] McDaniel et al., *The MR Cap: A single-sided MRI system designed for potential point-of-care limited field-of-view brain imaging*. Magn. Res. Med., 2019.
[3] Cooley et al., *Implementation of low-cost, instructional tabletop MRI scanners*. Int. Soc. Magn. Res. Med., 2014.
[4] Kuang et al., *Equivalent-Charge-Based Optimization of Spokes-and-Hub Magnets for Hand-Held and Classroom MR Imaging*. Int. Soc. Magn. Res. Med., 2019.

Permanent Magnet MR Imagers

- ✓Low cost
- ✓Portable
- ✓Safe for classroom and point-of-care use
- —Inhomogeneous compared to clinical scanners (<1 ppm over head)
- —Large negative temperature coefficient (thousands of ppm/°C)

Bloch Optimization of Dithered-Pulse RF

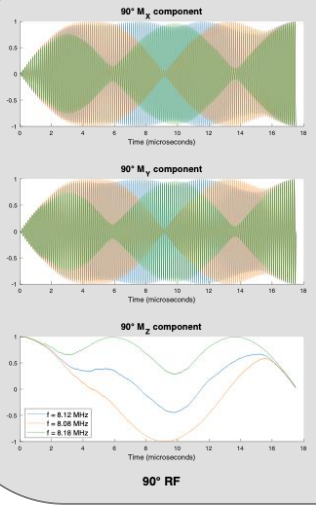

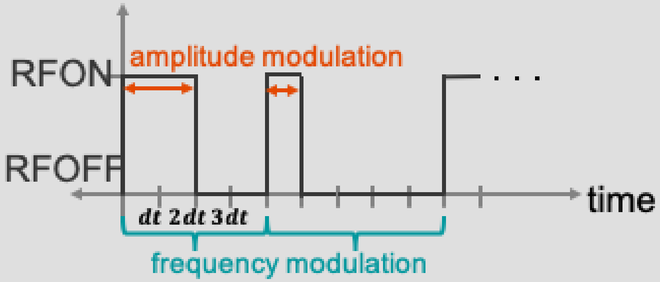

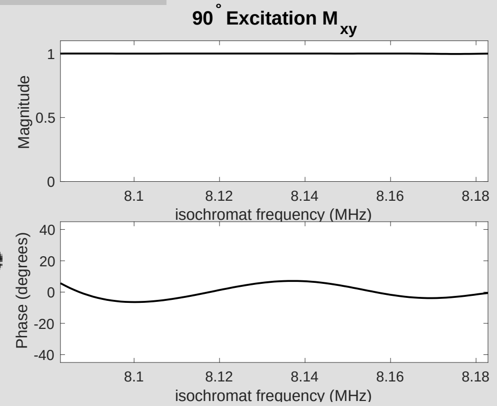

Low-Cost, Low-Field Inhomogeneous Permanent Magnet Imagers

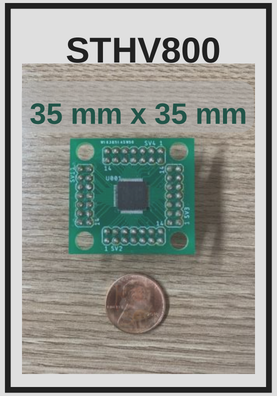

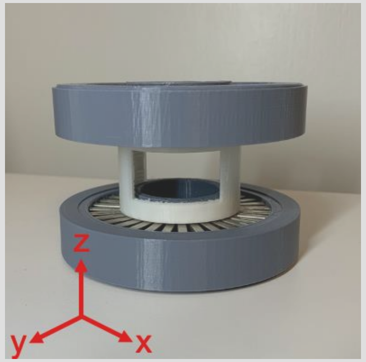

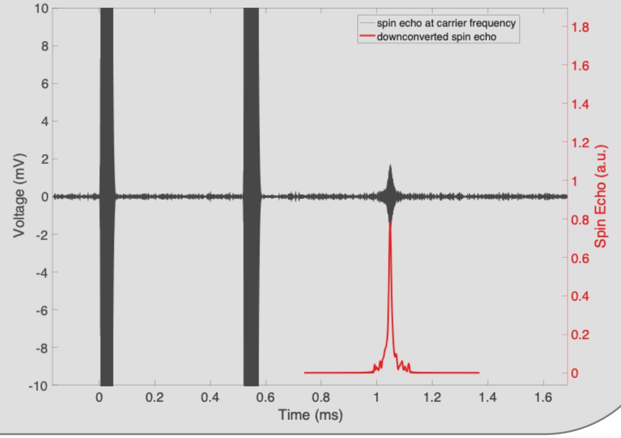

Low-Cost Ultrasound-Pulse RF Signal Chain

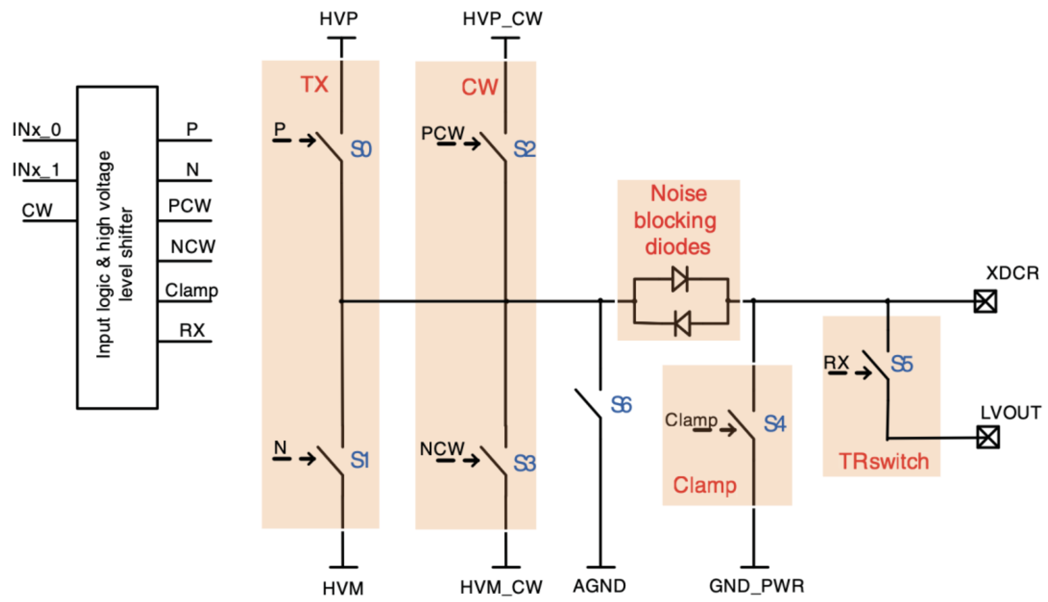

Single channel block diagram
Push-pull topology

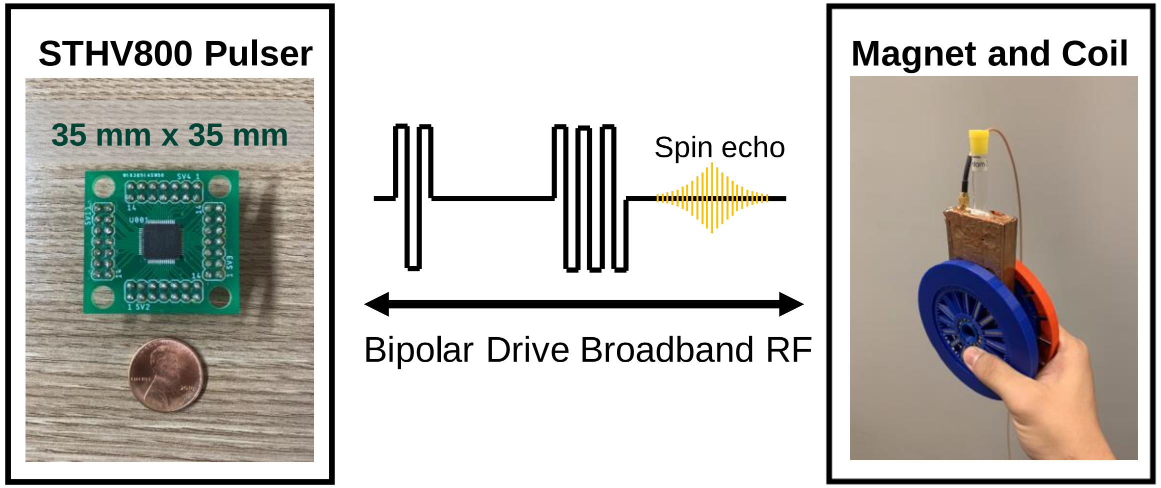

8-channel Ultrasound Pulser
STHV800: 30 USD

100-500 USD

Low-Cost Ultrasound-Pulse RF Signal Chain

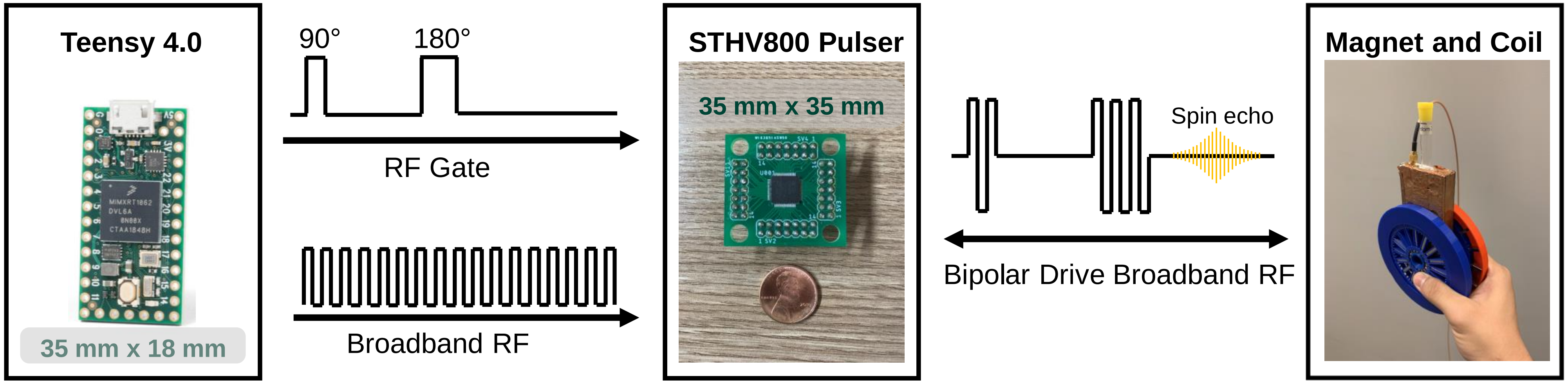

20 USD

8-channel Ultrasound Pulser
STHV800: 30 USD

100-500 USD

Dithered-Pulse RF Generation on Teensy 4.0

One digital output on Teensy 4.0 takes $dt = 3.33\ ns$

```
#define RFON digitalWriteFast(RF_ENV, true);
#define RFOFF digitalWriteFast(RF_ENV, false);
```

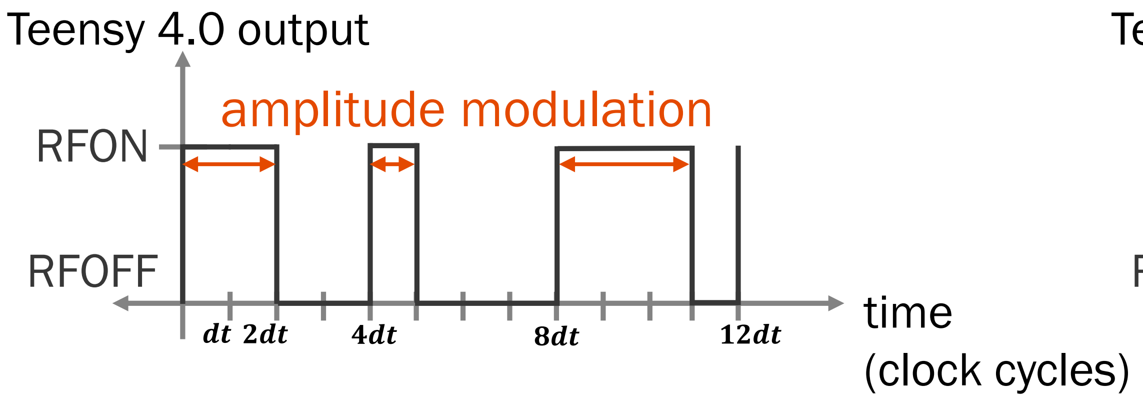

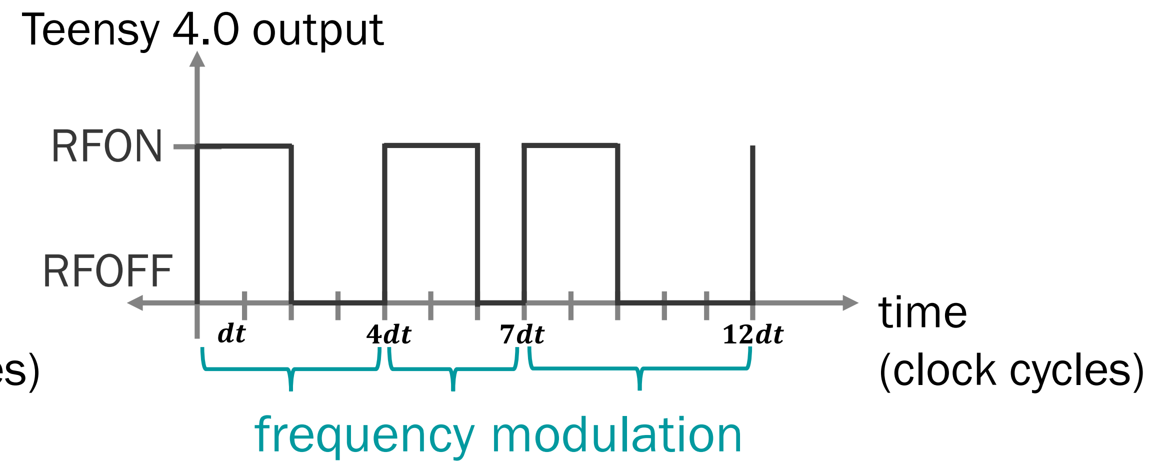

Dithered-Pulse RF Generation on Teensy 4.0

One digital output on Teensy 4.0 takes $dt = 3.33\ ns$

```
#define RFON digitalWriteFast(RF_ENV, true);
#define RFOFF digitalWriteFast(RF_ENV, false);
```

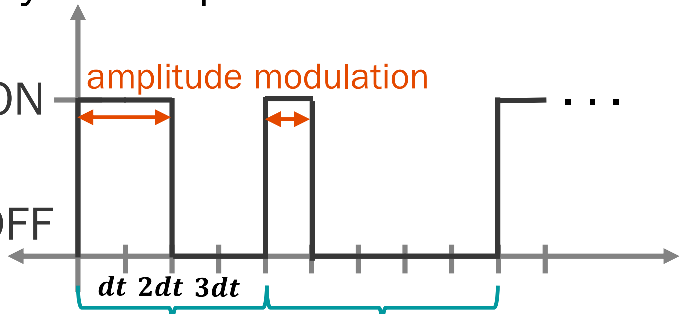

Optimizing for 90° flip

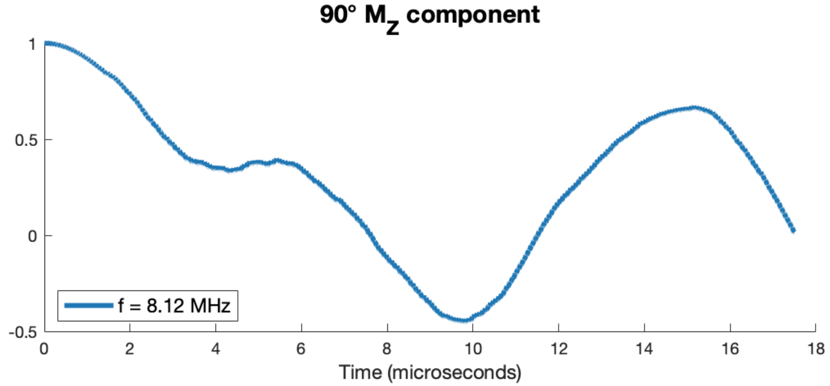

Dithered-pulse is a combination of **both** frequency and amplitude modulation

For a pulse centered at 8.13 MHz (B_0 = 191 mT):

- the number of digital write cycles (dt=3.33ns) required is 36.9
- optimizer is given 3 amplitude and 3 frequency modulation choices (9 total clock cycle combinations)

Nom B0=0.191 Nom Freq=8.1328

RFON→	18	19	20	19	20	21	19	20	21
RFOFF→	18	17	16	18	17	16	19	18	17

Bloch Equation Simulation Approach

$$\frac{d}{dt}\begin{pmatrix} M_x \\ M_y \\ M_z \end{pmatrix} = \begin{pmatrix} -\frac{1}{T_2} & \gamma B_z & -\gamma B_y \\ -\gamma B_z & -\frac{1}{T_2} & \gamma B_x \\ \gamma B_y & -\gamma B_x & -\frac{1}{T_1} \end{pmatrix}\begin{pmatrix} M_x \\ M_y \\ M_z \end{pmatrix} + \begin{pmatrix} 0 \\ 0 \\ \frac{M_0}{T_1} \end{pmatrix}$$

Apply RF pulse in transverse plane

$$\frac{d}{dt}\begin{pmatrix} M_x \\ M_y \\ M_z \end{pmatrix} = \begin{pmatrix} -1 & \gamma B_z & \\ -\gamma B_z & -1 & \gamma B_x \\ & -\gamma B_x & -1 \end{pmatrix}\begin{pmatrix} M_x \\ M_y \\ M_z \end{pmatrix} + \begin{pmatrix} 0 \\ 0 \\ M_0 \end{pmatrix}$$

Precompute $\boldsymbol{M}$

- for all frequency/amplitude modulation combinations
- for all B_0 isochromats within a desired frequency bandwidth

Optimize dithered square-wave pulse to flip spins with Matlab genetic algorithm

[5] Wimperis, S., *Broadband, Narrowband, and Passband Composite Pulses for Use in Advanced NMR Experiments*. J. Magn. Res., 1994.
[6] Garwood et al., *The Return of the Frequency Sweep: Designing Adiabatic Pulses for Contemporary NMR.* J. Magn. Res., 2001.
[7] Maximov et al., *Optimal control design of NMR and dynamic nuclear polarization experiments using monotonically convergent algorithms*. J. Chem. Phys., 2008.

90° Bloch Simulation Result

Spin evolution of M_x, M_y, M_z component for 1 isochromat (at 8.12 MHz)

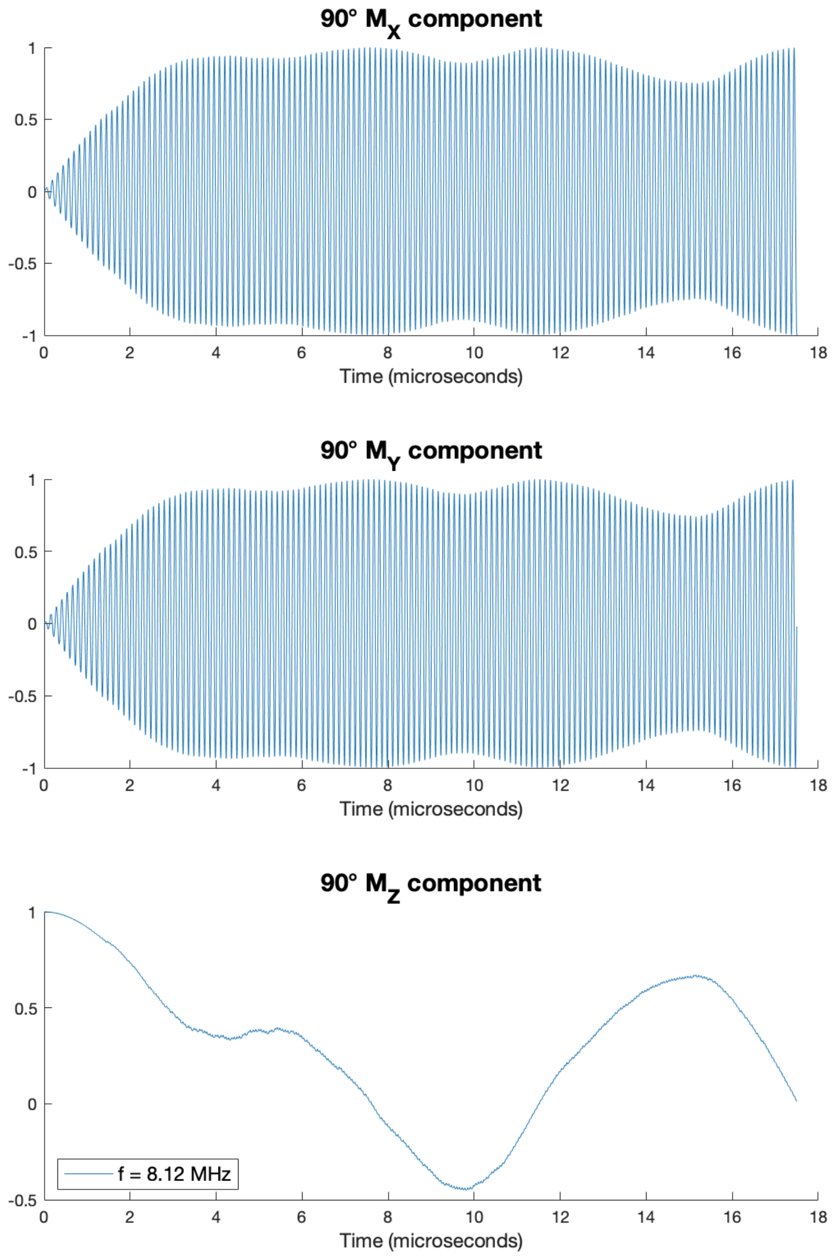

90° RF

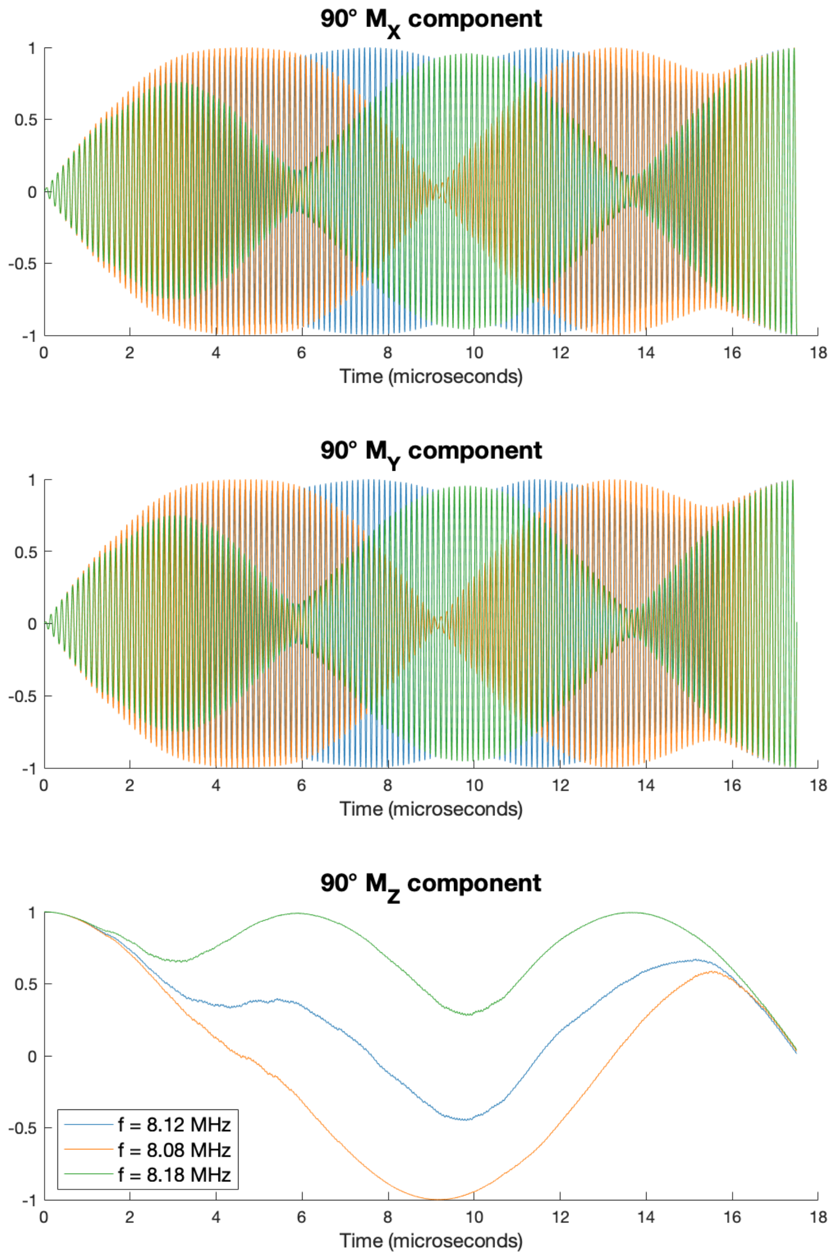

90° RF

90° Bloch Simulation Result

Spin evolution of M_x, M_y, M_z component for 3 isochromats (from 8.08–8.18 MHz)

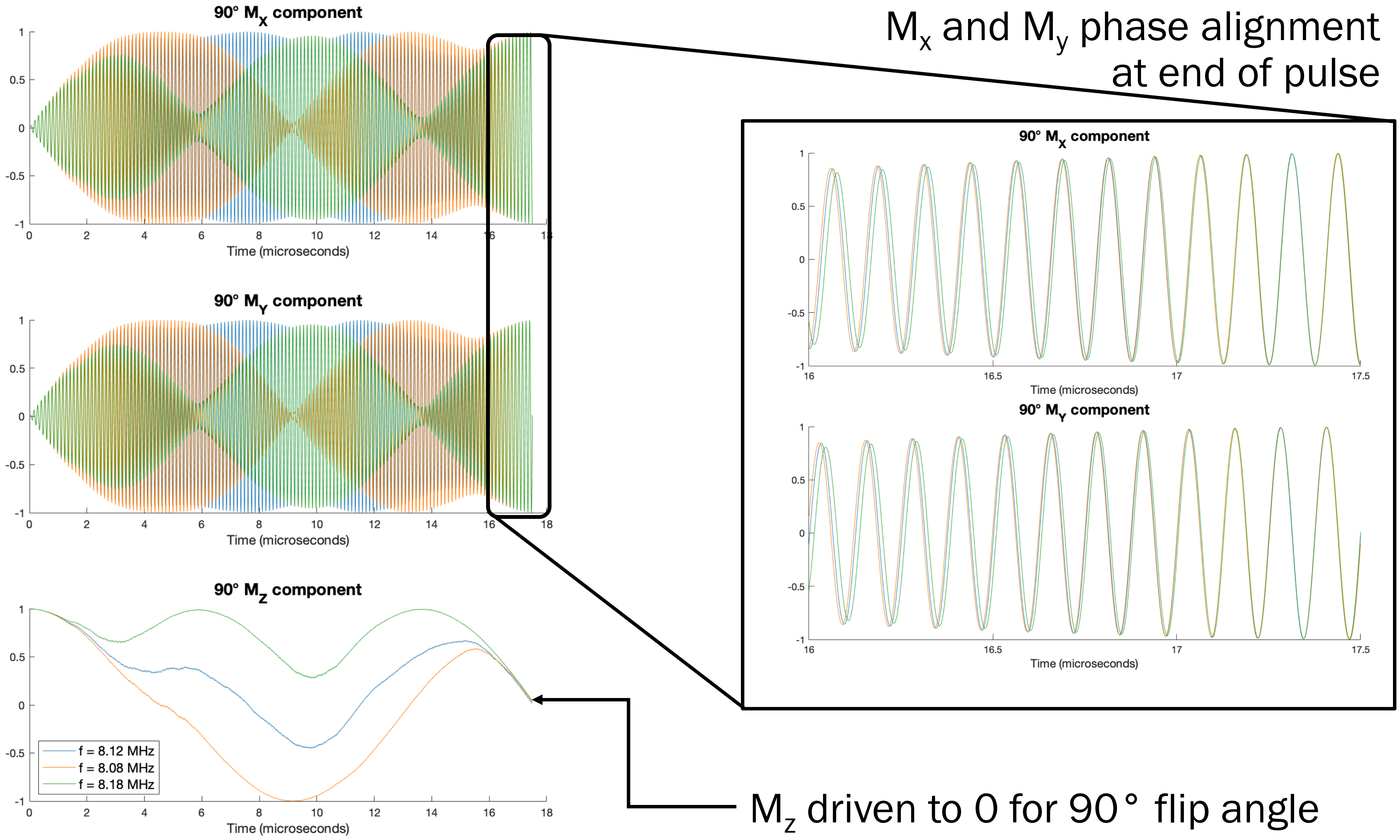

Mx and My phase alignment at end of pulse
90° MX component
90° MY component
90° MZ component
Time (microseconds)
f = 8.12 MHz
f = 8.08 MHz
f = 8.18 MHz
Mz driven to 0 for 90° flip angle

90° RF

90° Bloch Simulation Result

- Each isochromat curve represents magnetization (M_x, M_y, M_z) of one frequency within an optimized 100 kHz bandwidth
- Phase alignment of M_x and M_y frequency isochromats at the end of pulse
- 90° flip of M_z

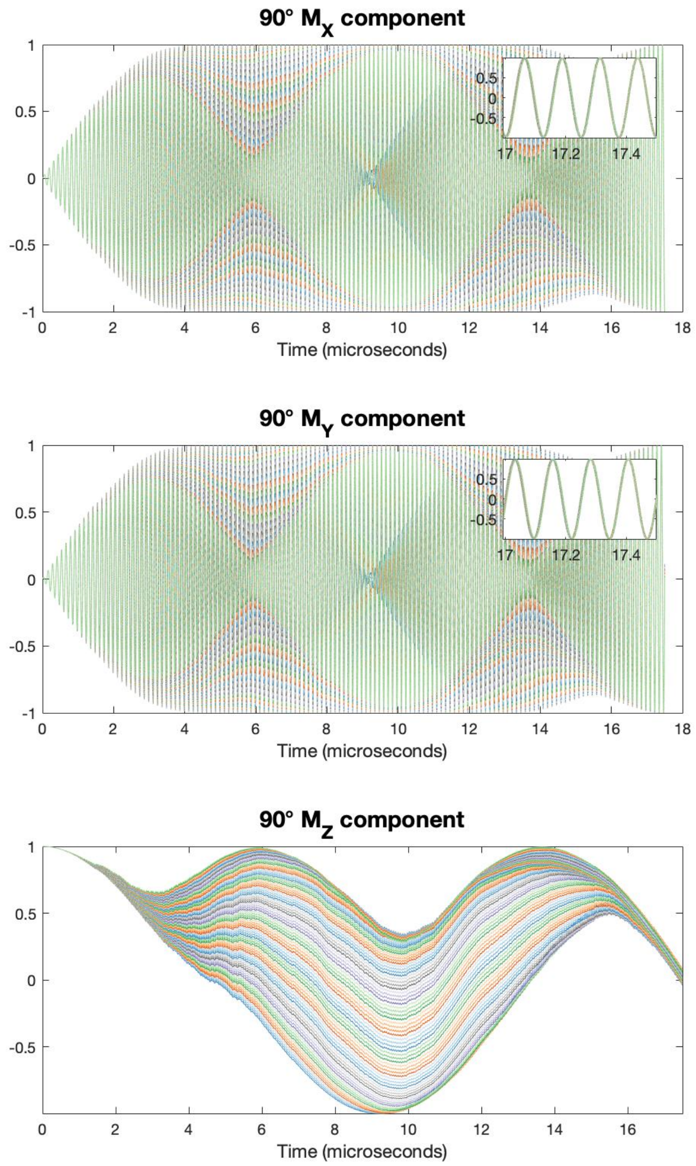

90° RF

Magnitude and phase for Mx My

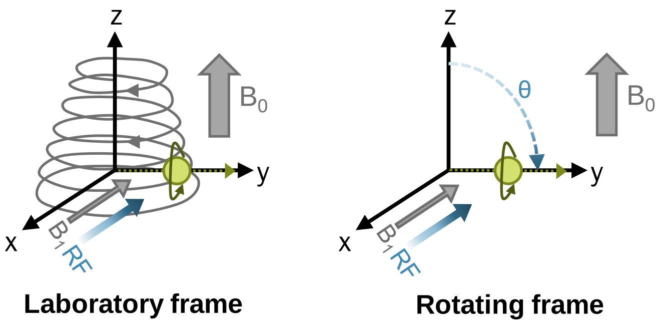

90° Bloch Simulation Result

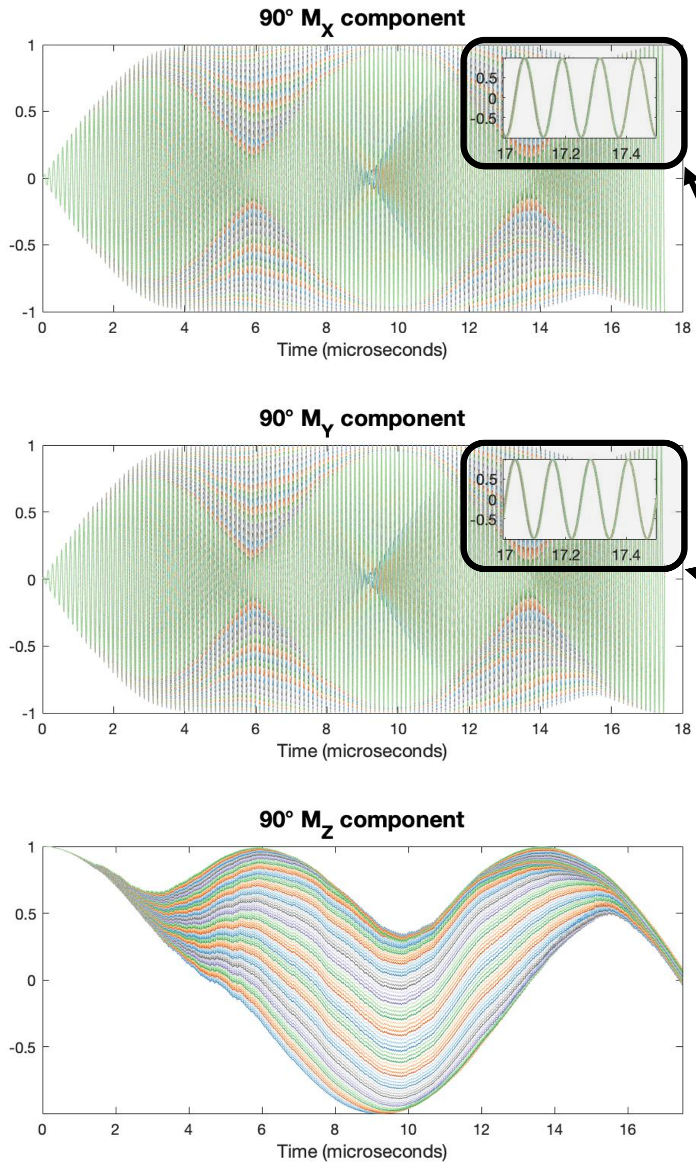

90° RF

- Each isochromat curve represents magnetization (M_x, M_y, M_z) of one frequency within an optimized 100 kHz bandwidth
- Phase alignment of M_x and M_y frequency isochromats at the end of pulse
- 90° flip of M_z

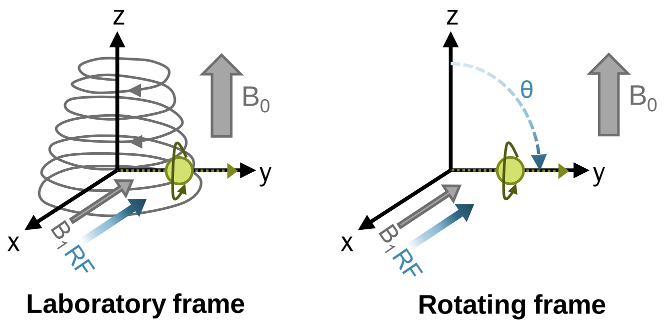

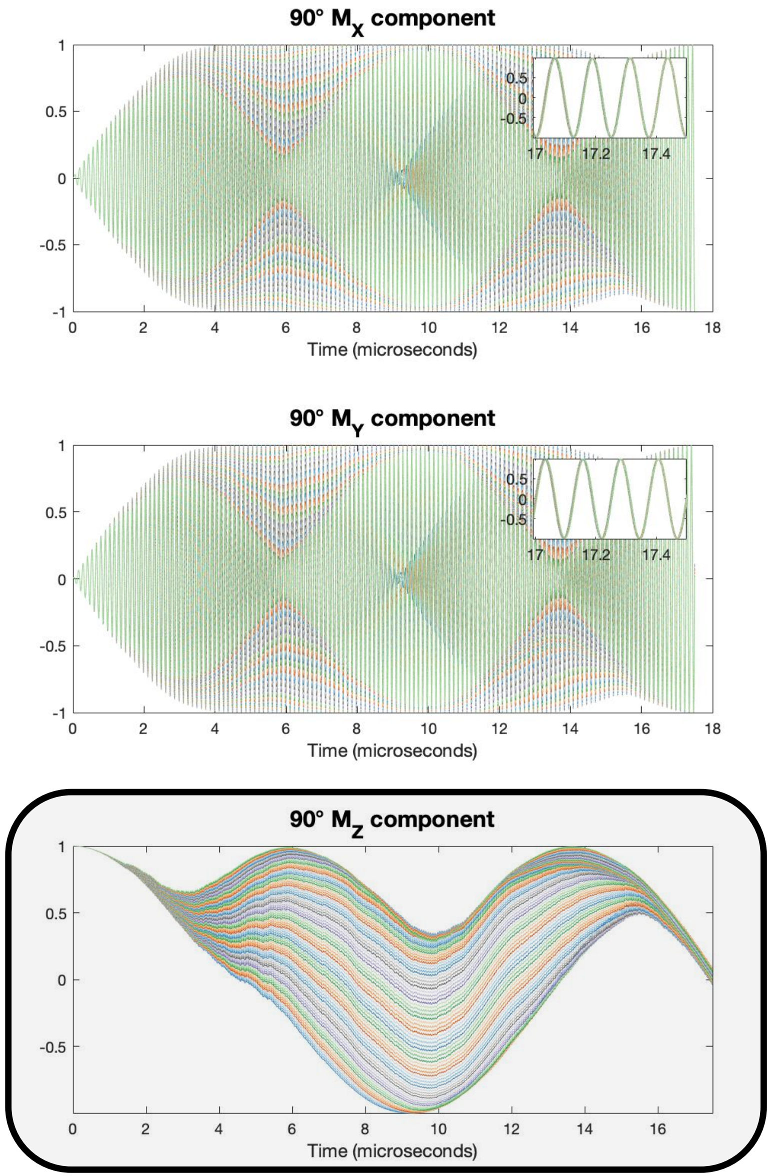

90° RF

90° Bloch Simulation Result

- Each isochrone curve represents magnetization (M_x, M_y, M_z) of one frequency within an optimized 100 kHz bandwidth
- Phase alignment of M_x and M_y frequency isochrones at the end of pulse
- 90° flip of M_z

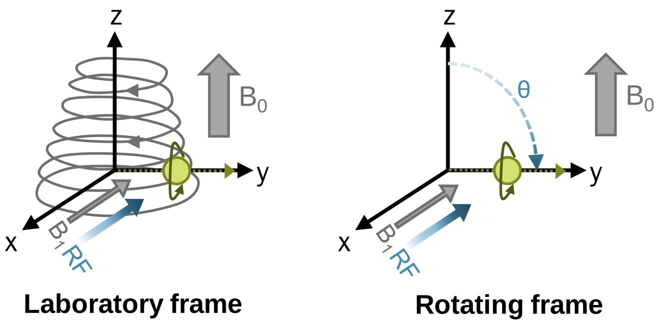

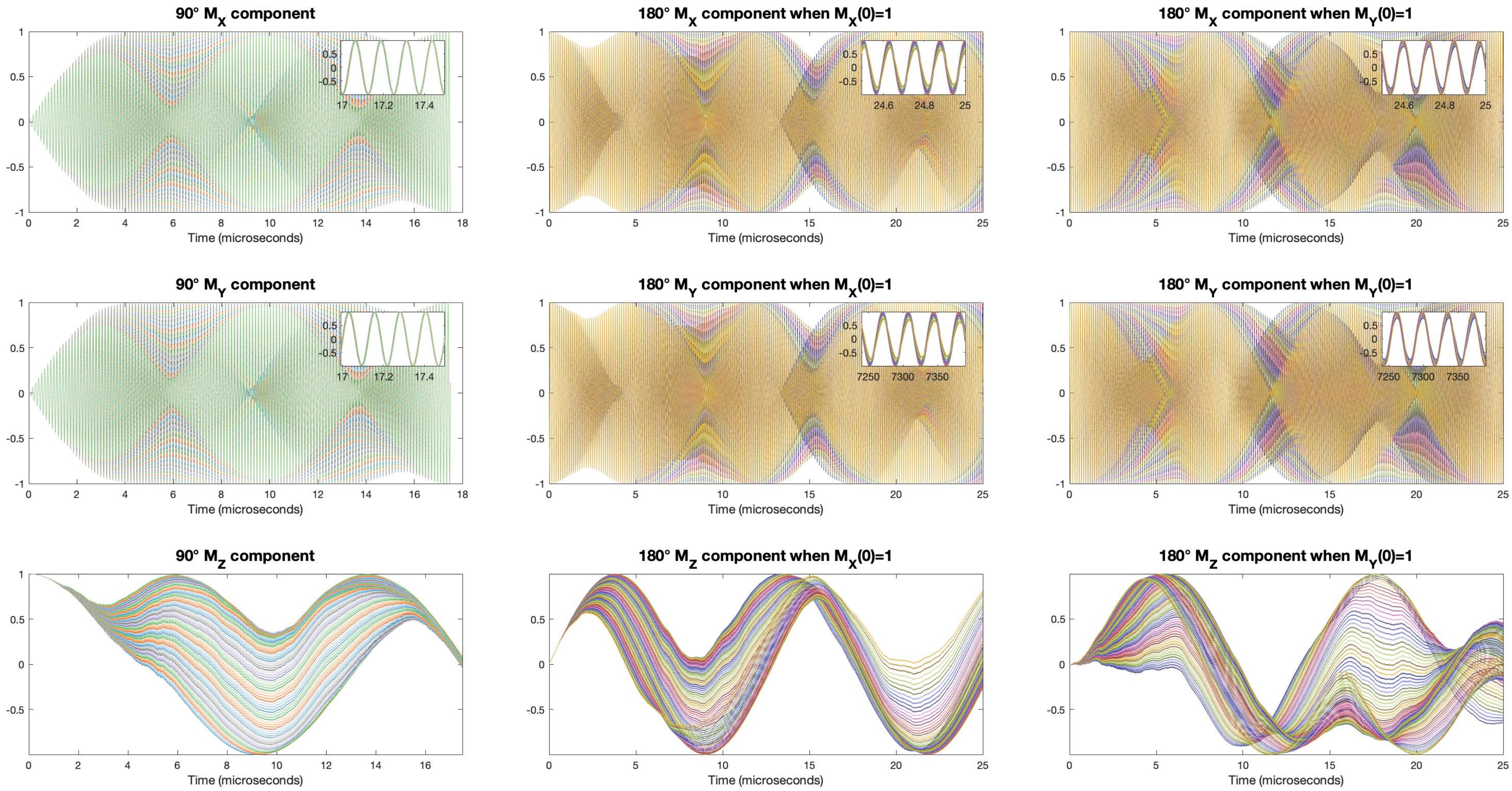

90° RF | **180° RF, $M_X(0)=1$** | **180° RF, $M_Y(0)=1$**

Optimized Dithered-Pulse Simulation

Amplitude- and Frequency-modulated dithered-pulse

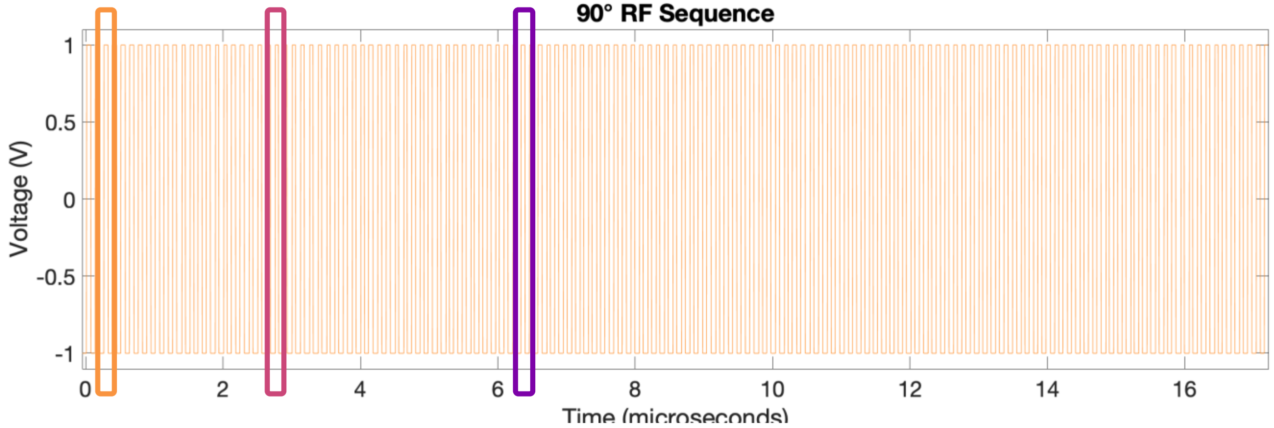

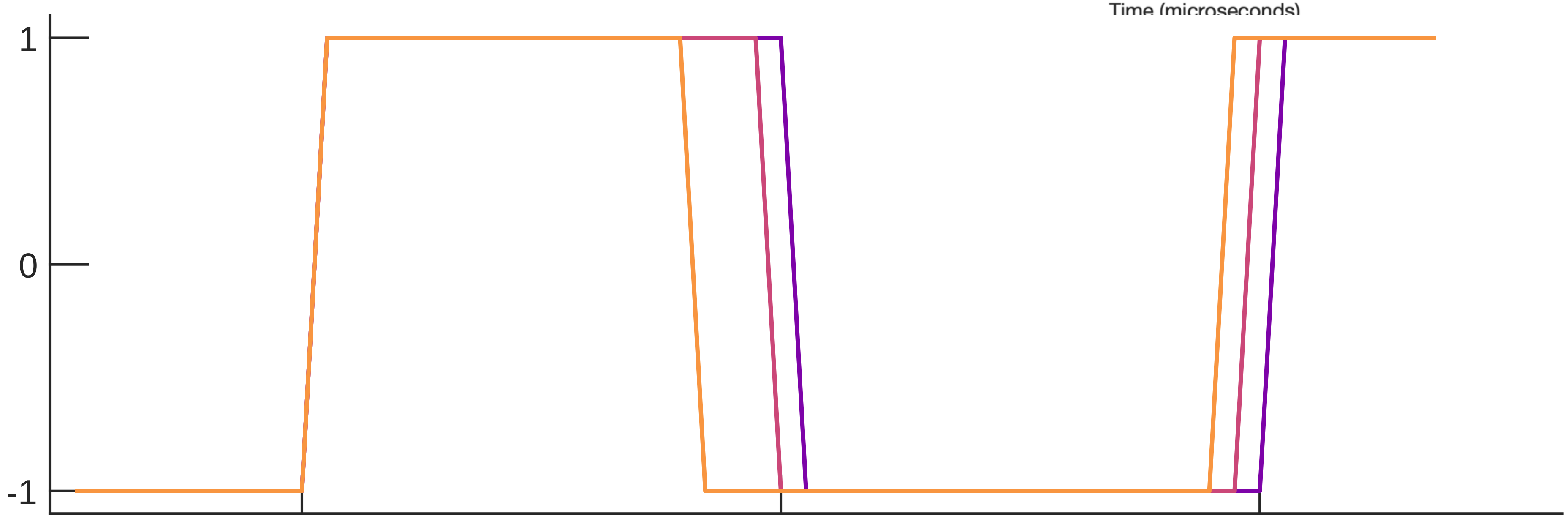

start of aligned period

Optimized Dithered-Pulse Simulation

Amplitude- and Frequency-modulated dithered-pulse

Spectrum of pulse

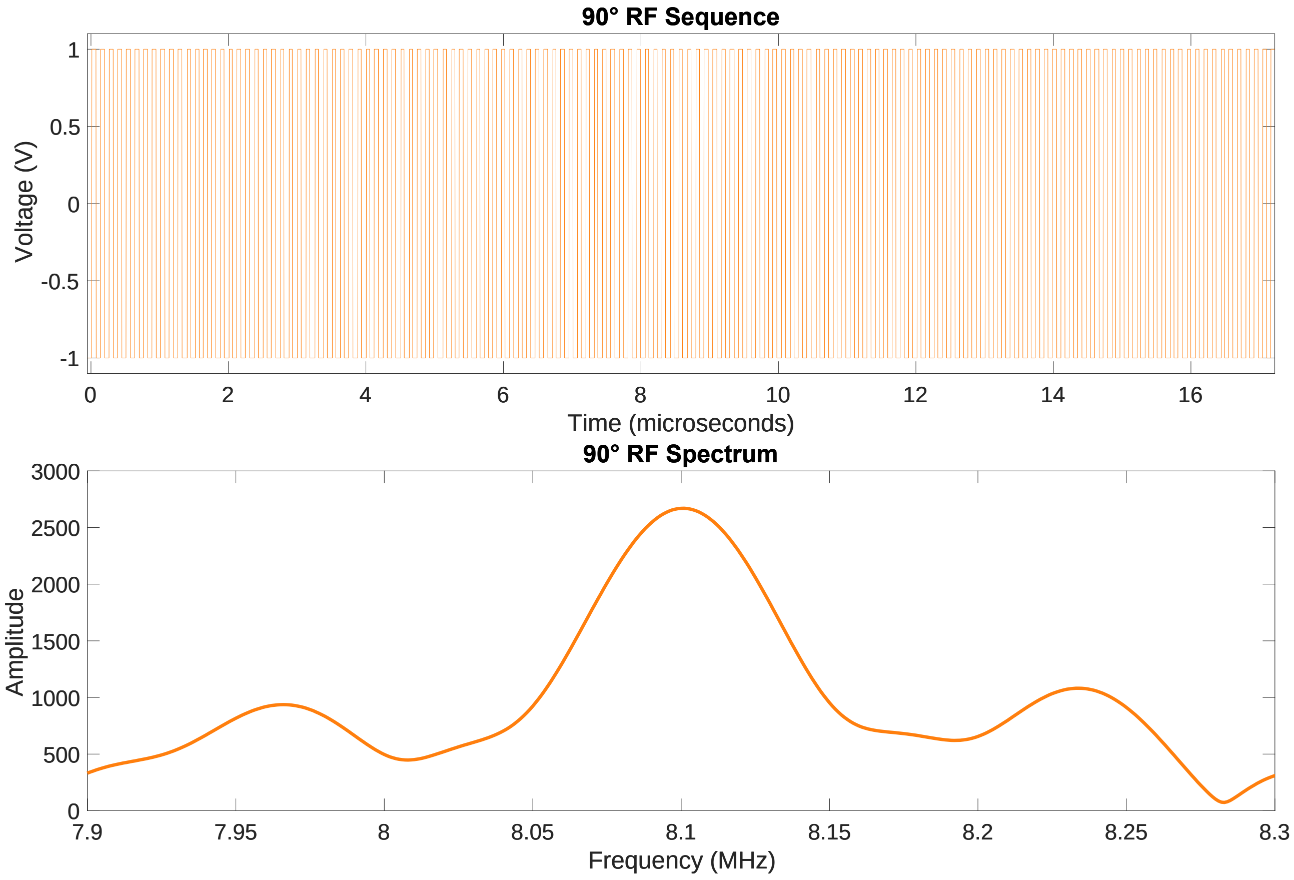

100 kHz optimization bandwidth

Optimized Dithered-Pulse Simulation

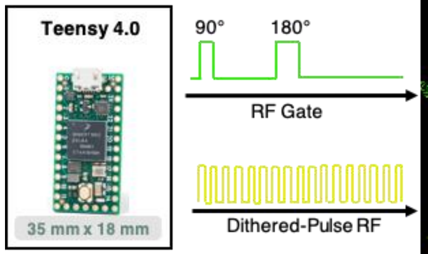

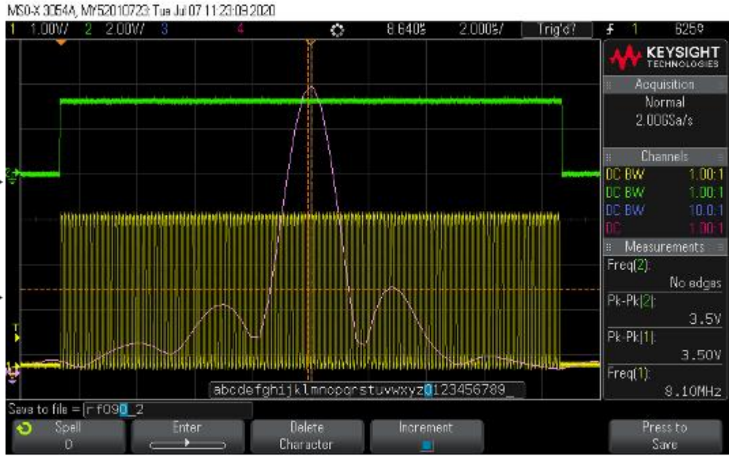

Oscilloscope FFT of pulse

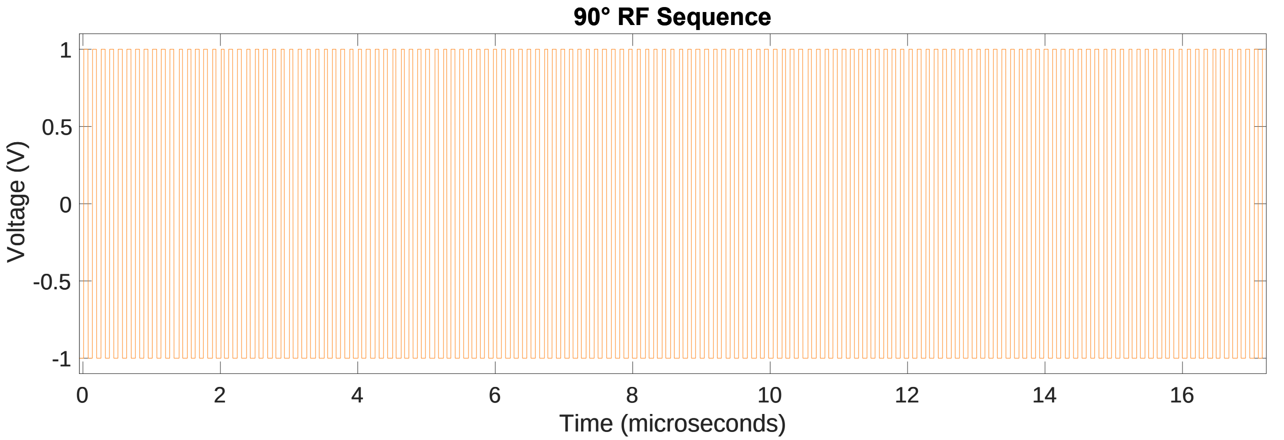

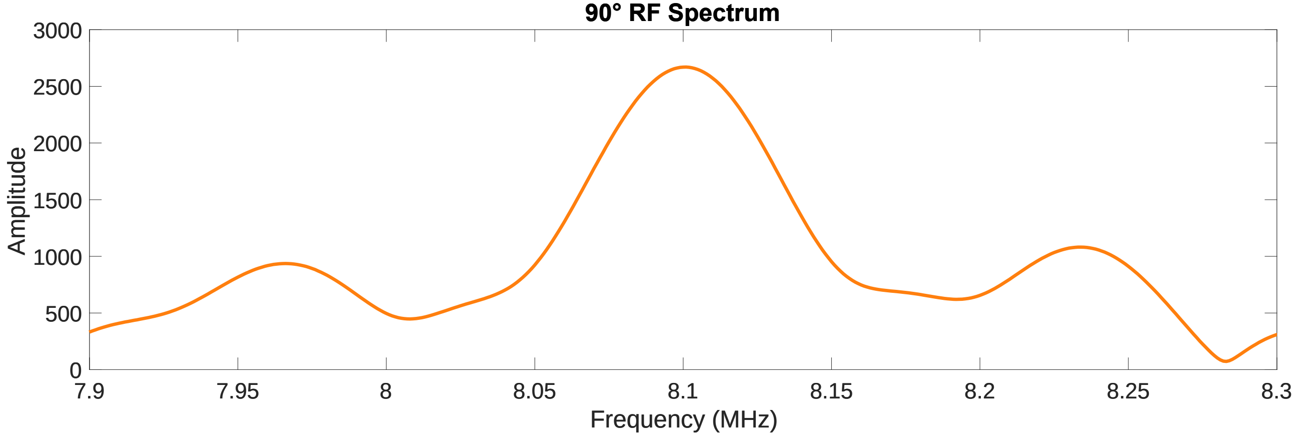

100 kHz optimization bandwidth

Accurate Reproduction of Pulse on Hardware

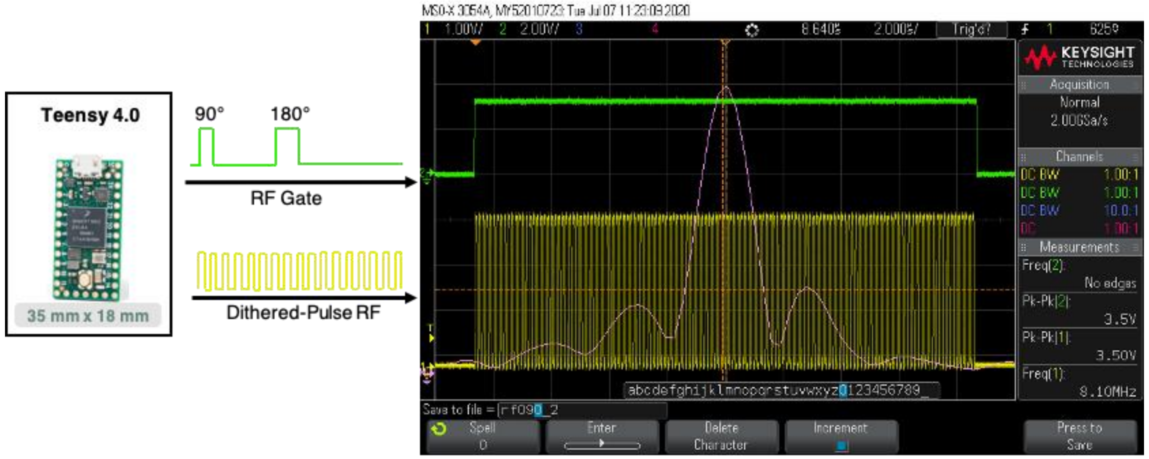

Oscilloscope FFT of pulse

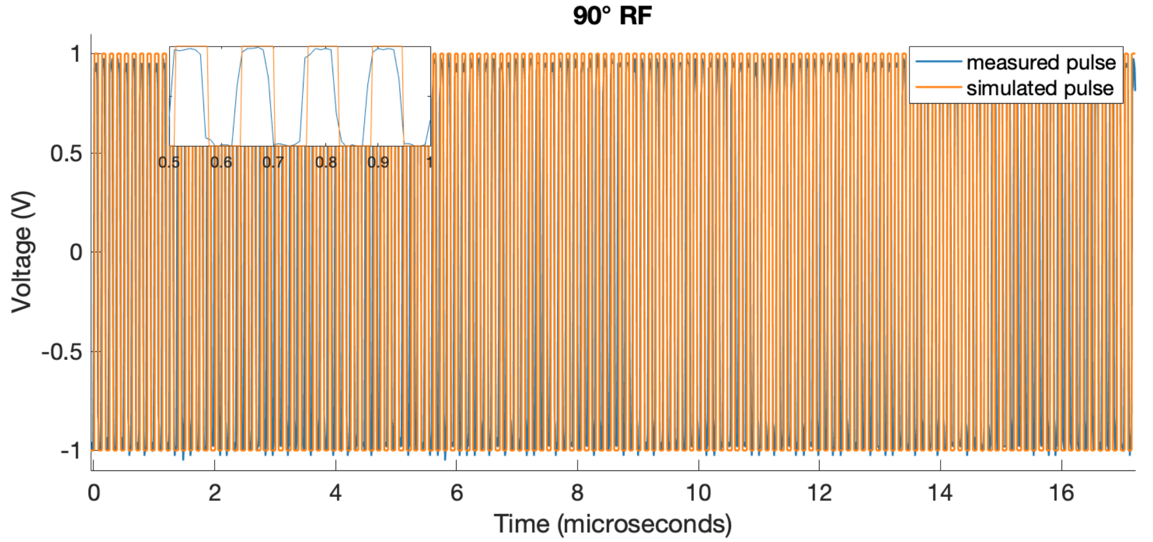

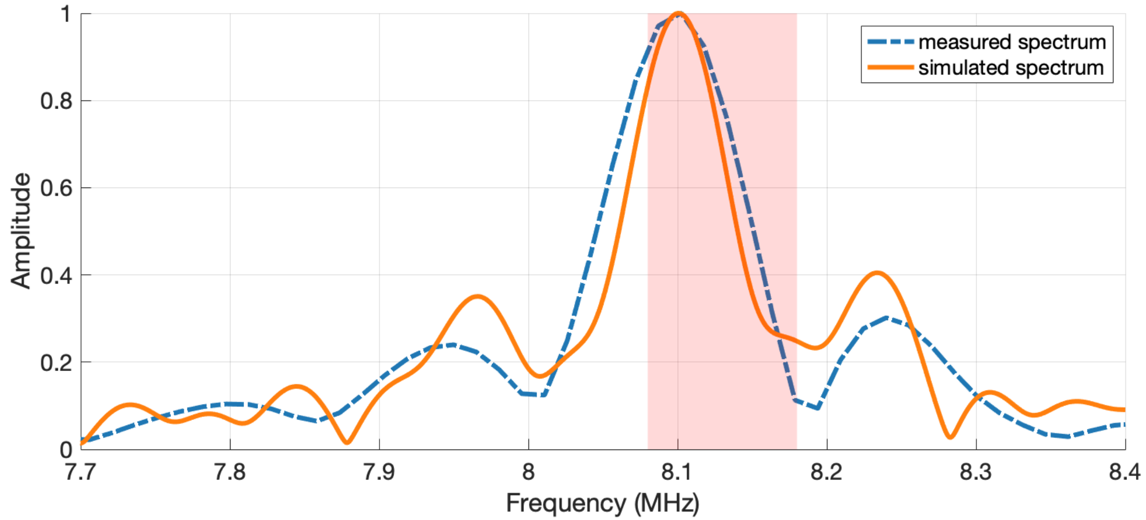

100 kHz optimization bandwidth

Magnitude and Phase of M_{xy} at end of 90°

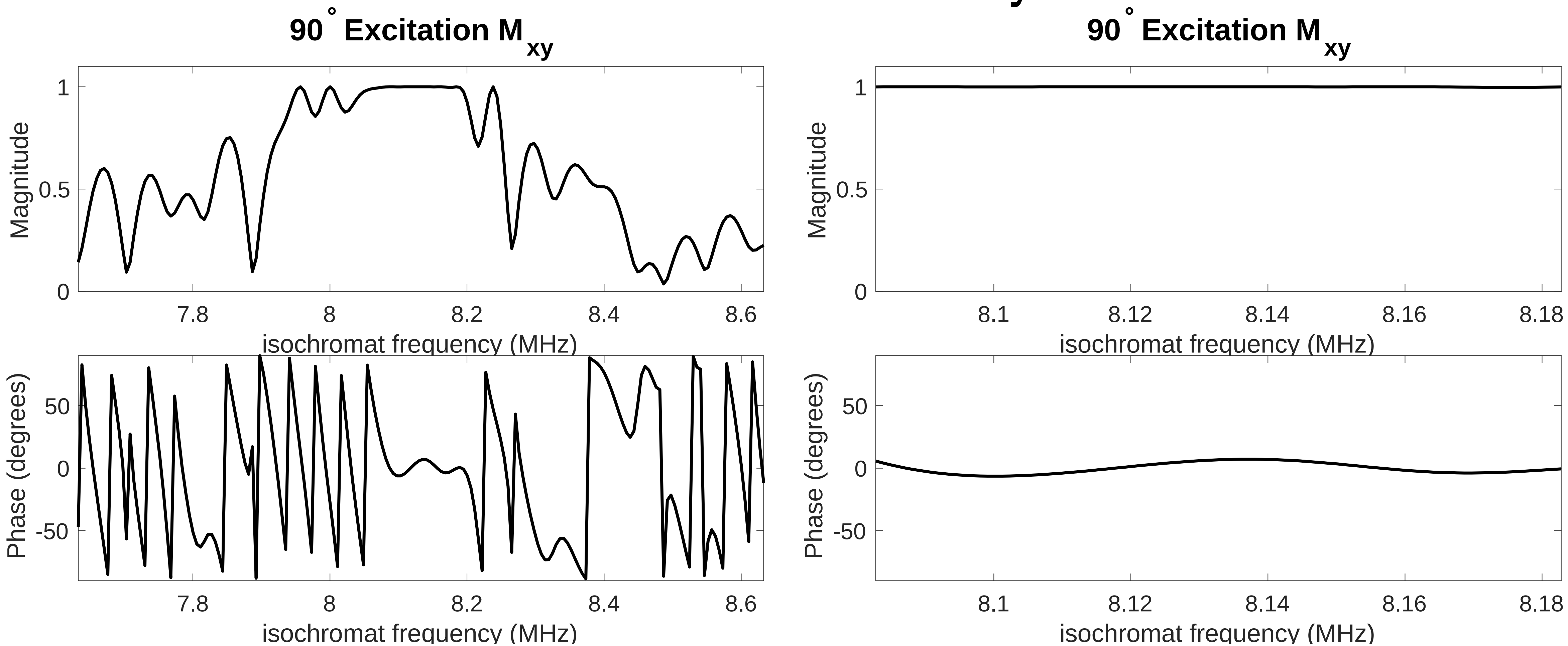

100 kHz optimization bandwidth

Magnitude and Phase of M_{xy} at end of 180°

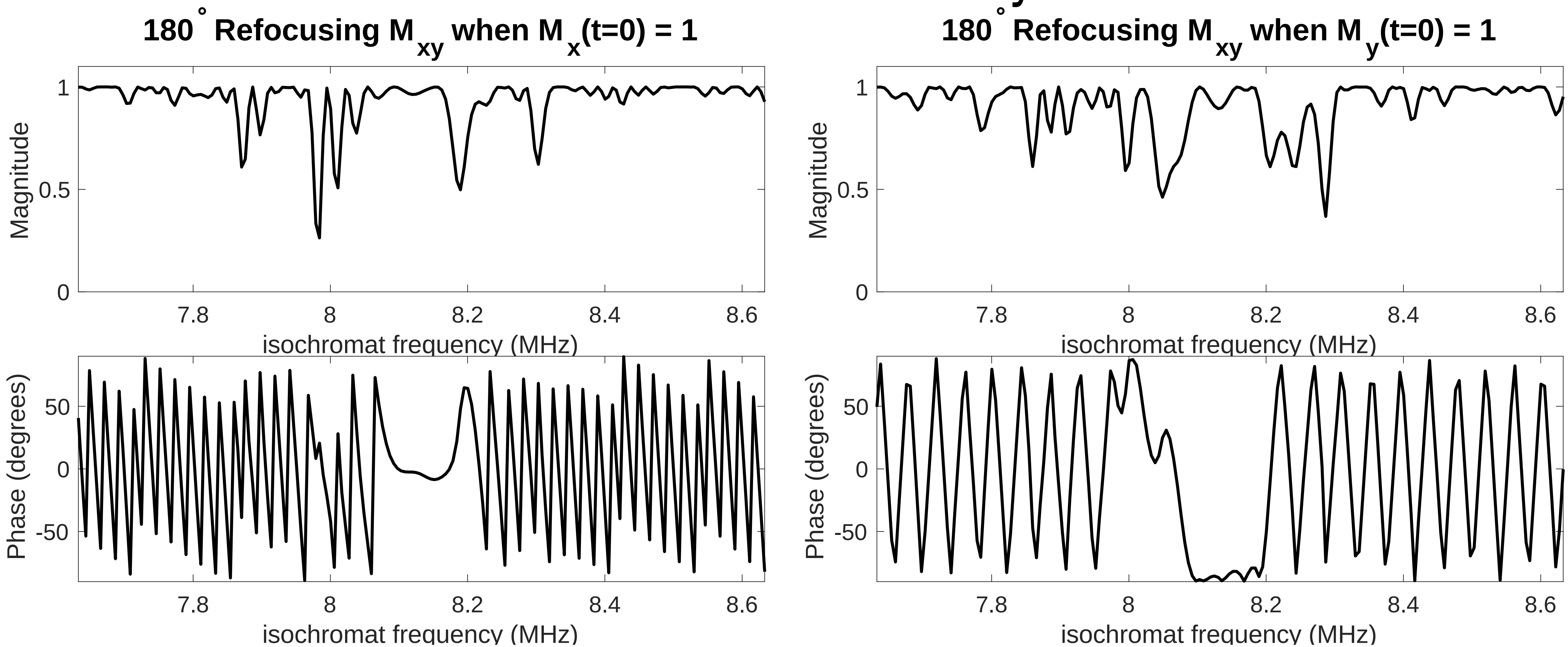

100 kHz optimization bandwidth

Initial Phase = 0°
$M_x(t=0) = 1$

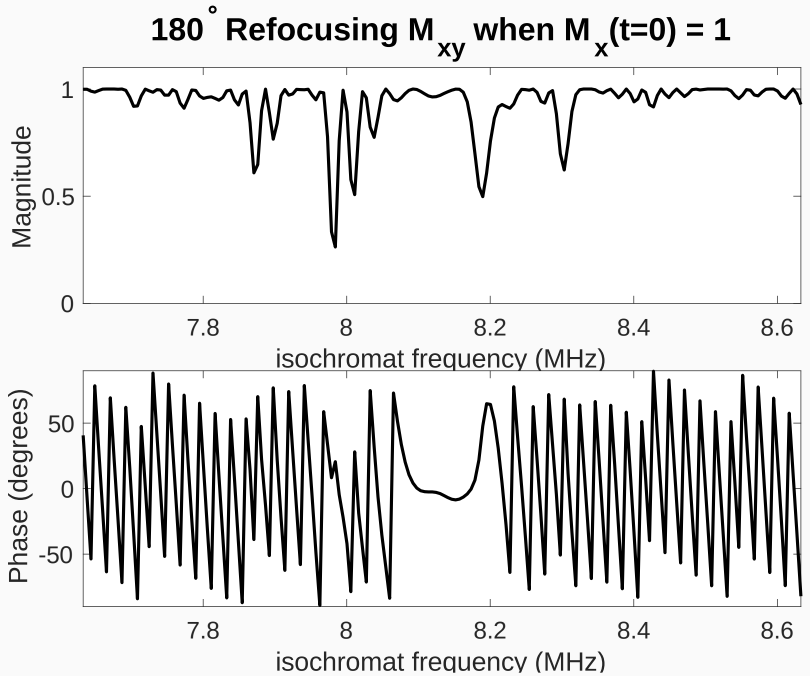

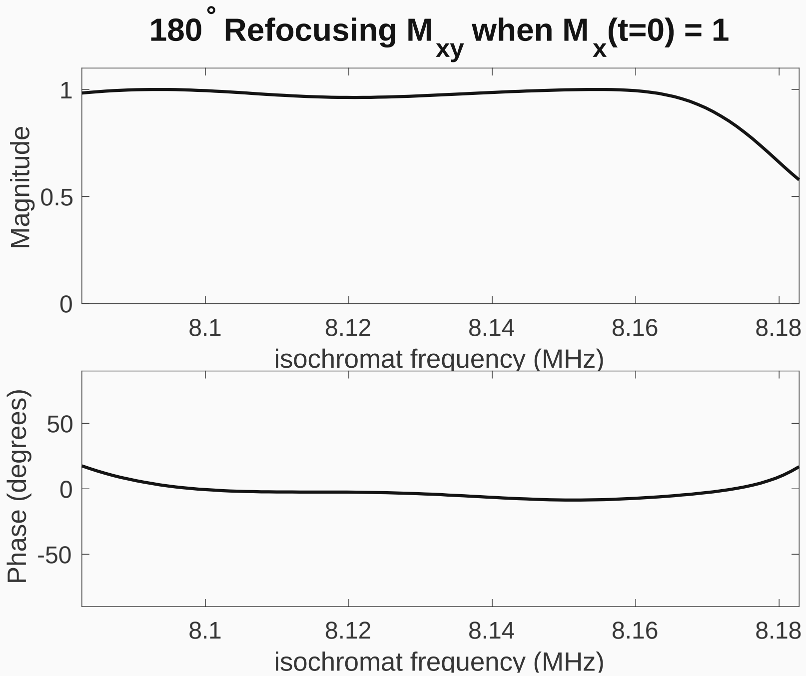

Initial Phase = 90°
$M_y(t=0) = 1$

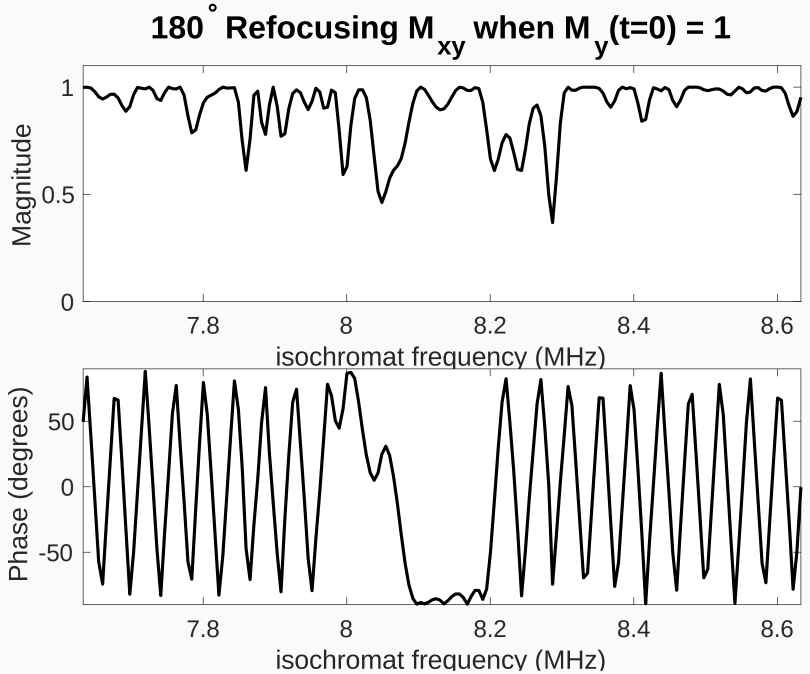

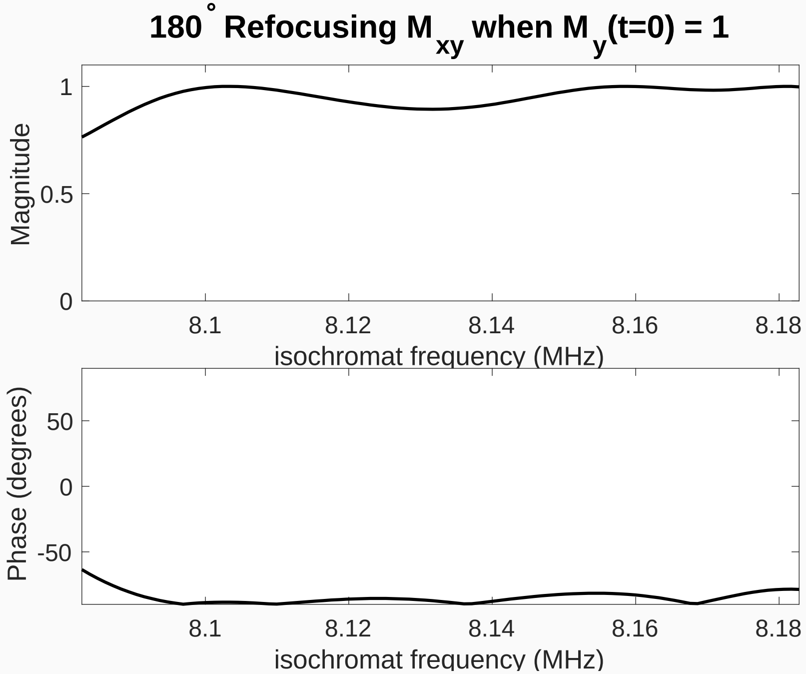

Spokes-and-hub permanent magnet array

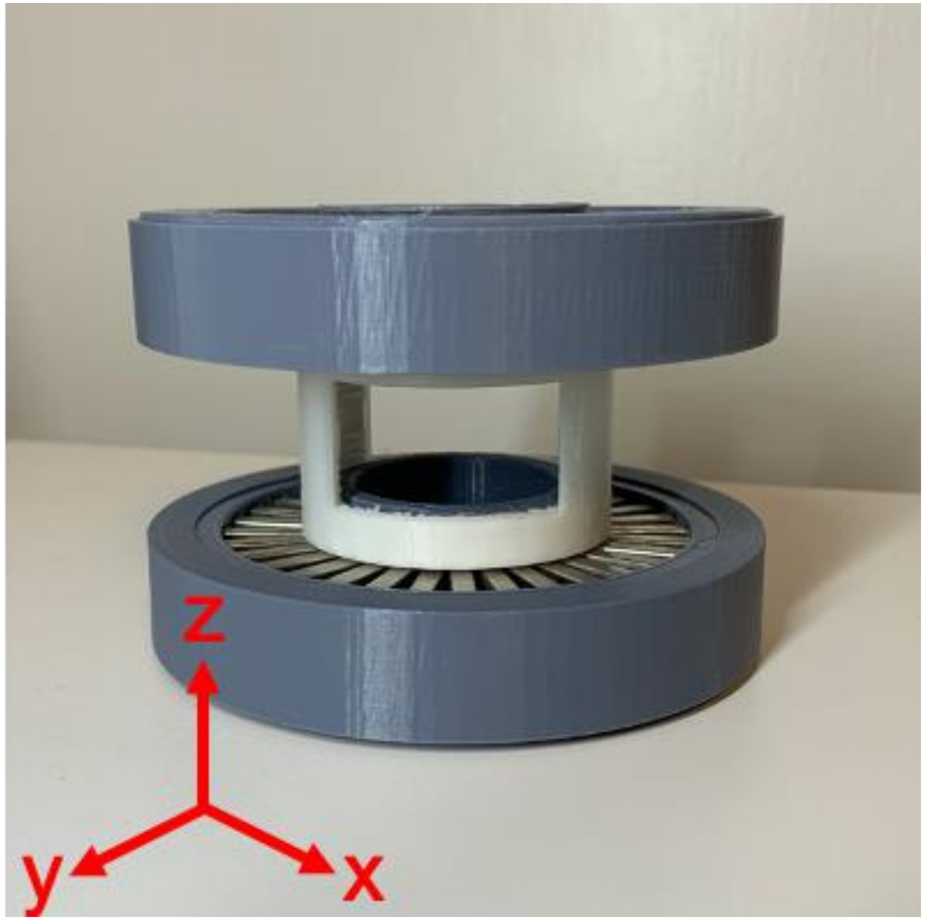

[4] Kuang et al., *Equivalent-Charge-Based Optimization of Spokes-and-Hub Magnets for Hand-Held and Classroom MR Imaging*. Int. Soc. Magn. Res. Med., 2019.

Field variation in permanent magnet array

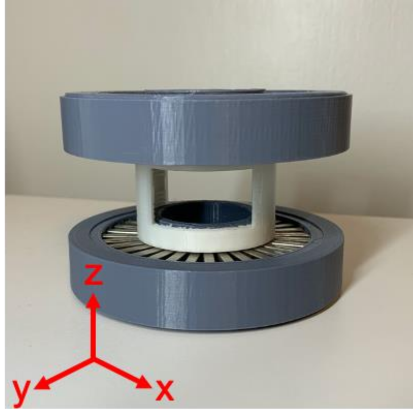

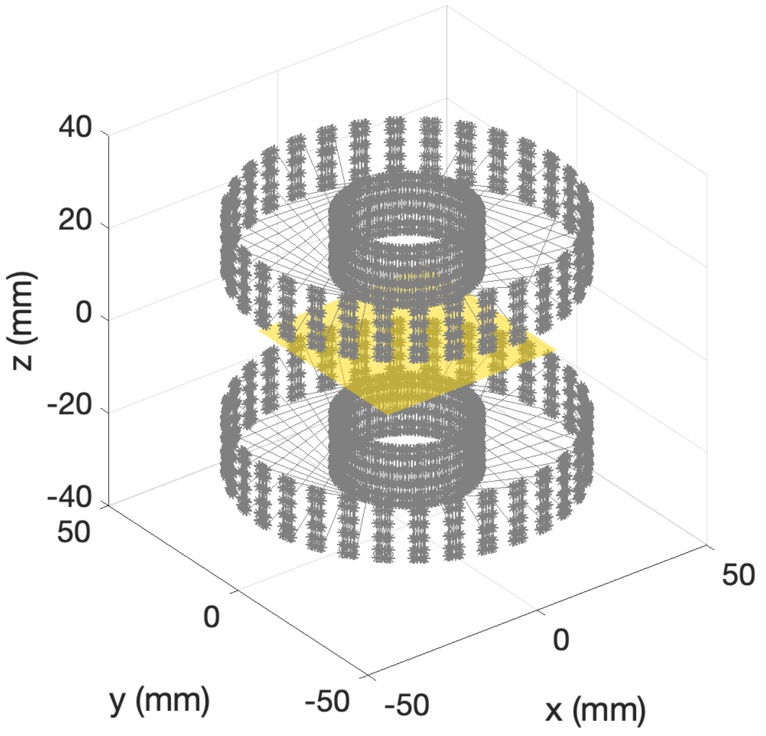

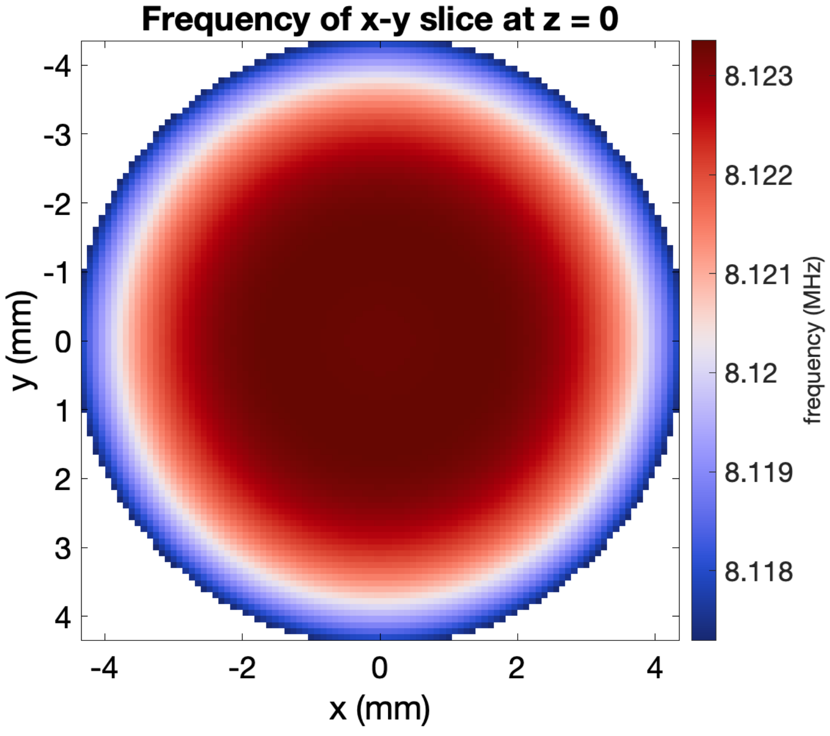

Radially symmetric fields

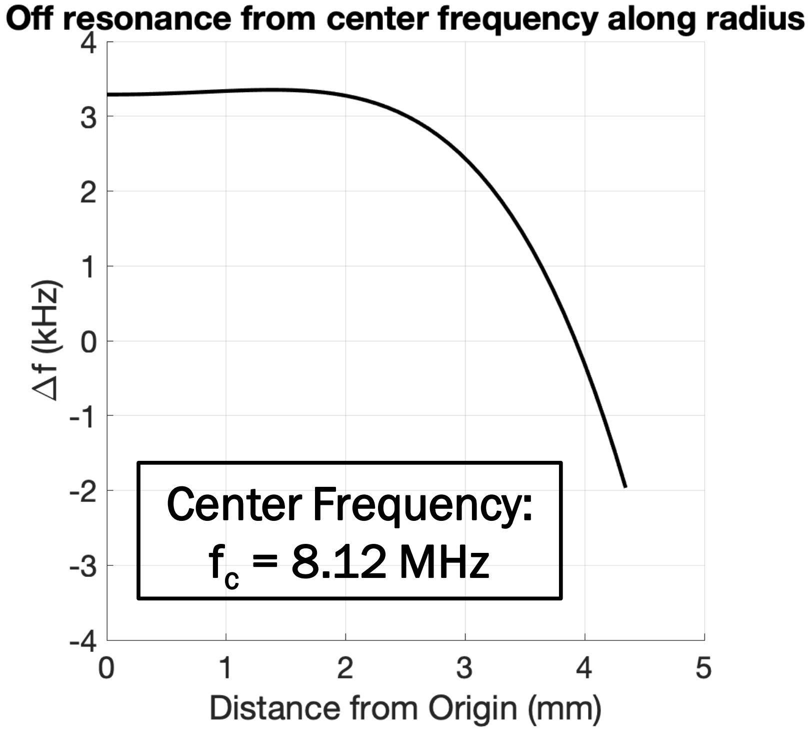

5 kHz bandwidth

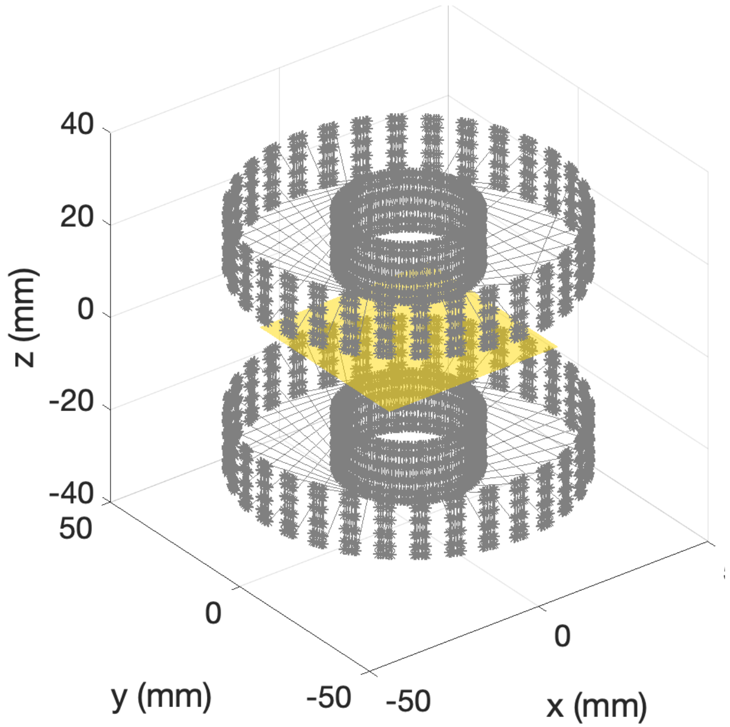

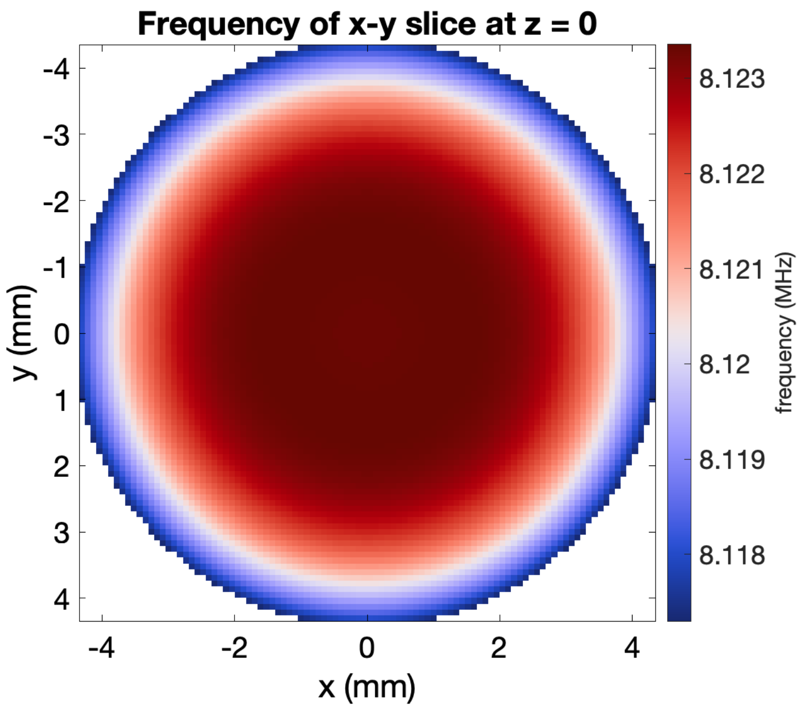

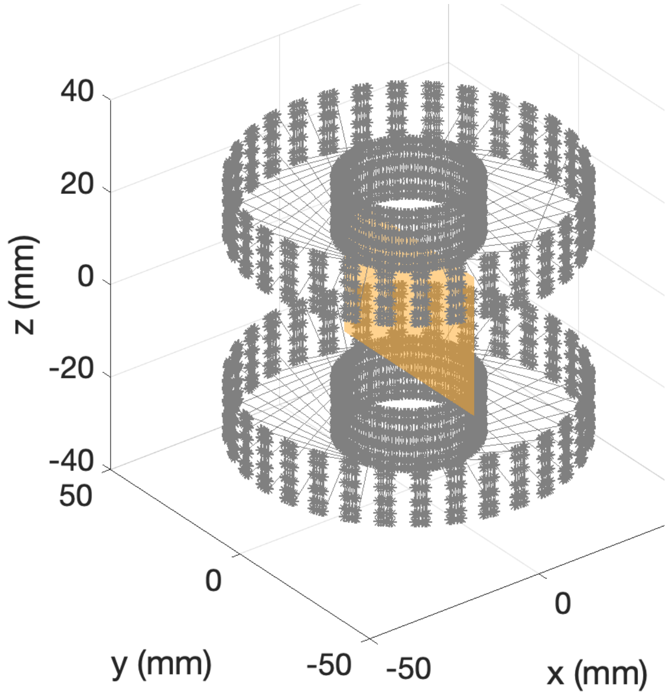

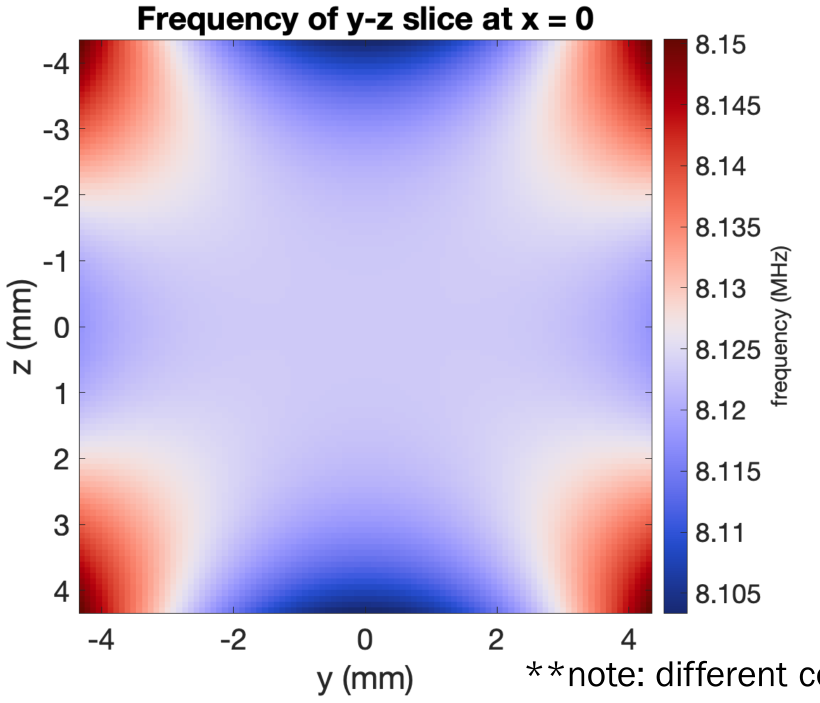

<u>Bandwidth of 8x8x8 mm volume:</u>
x-y slice: ±2.5 kHz
y-z slice: ±25 kHz

**note: different colorbar scales

Full RF Signal Chain

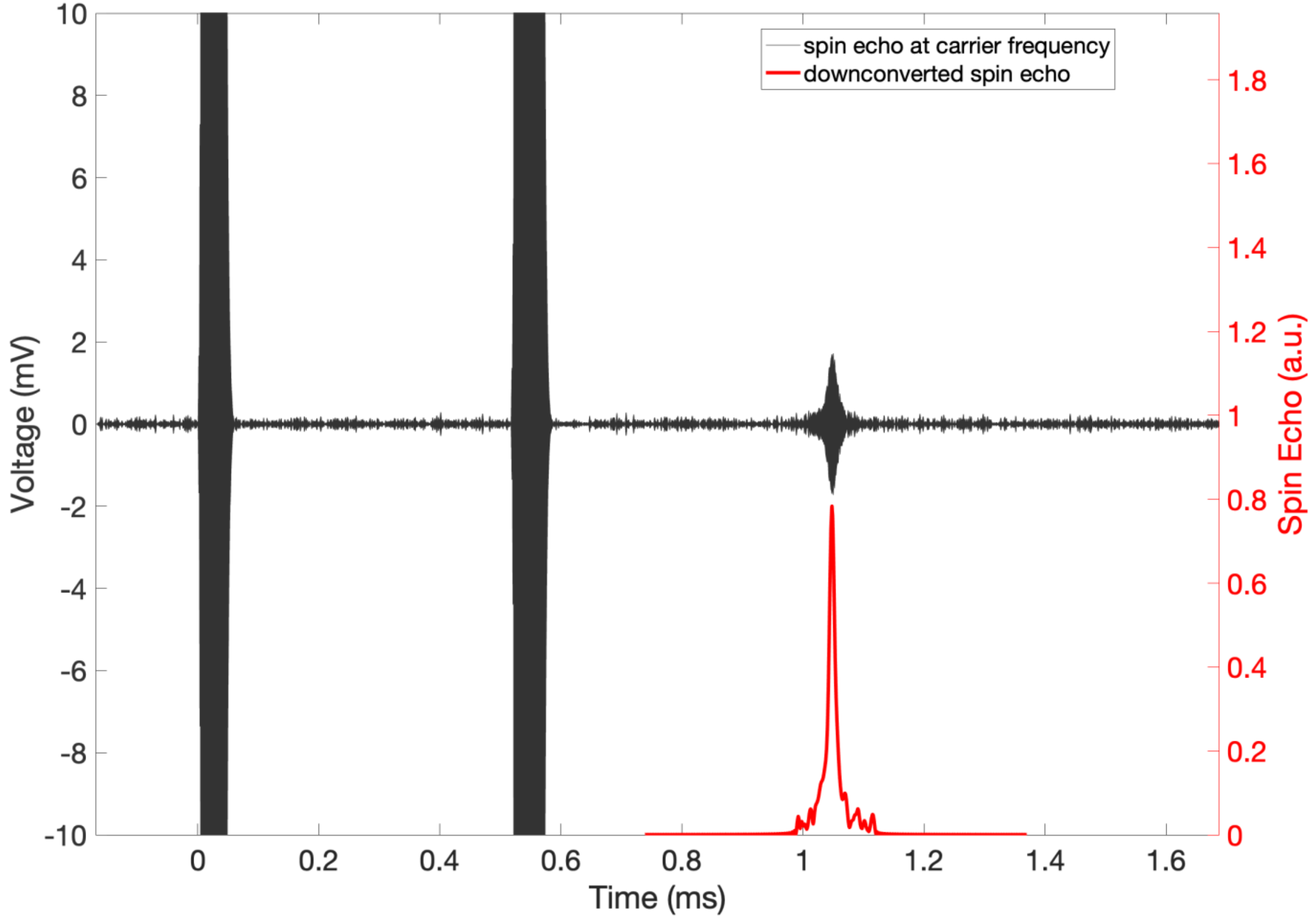

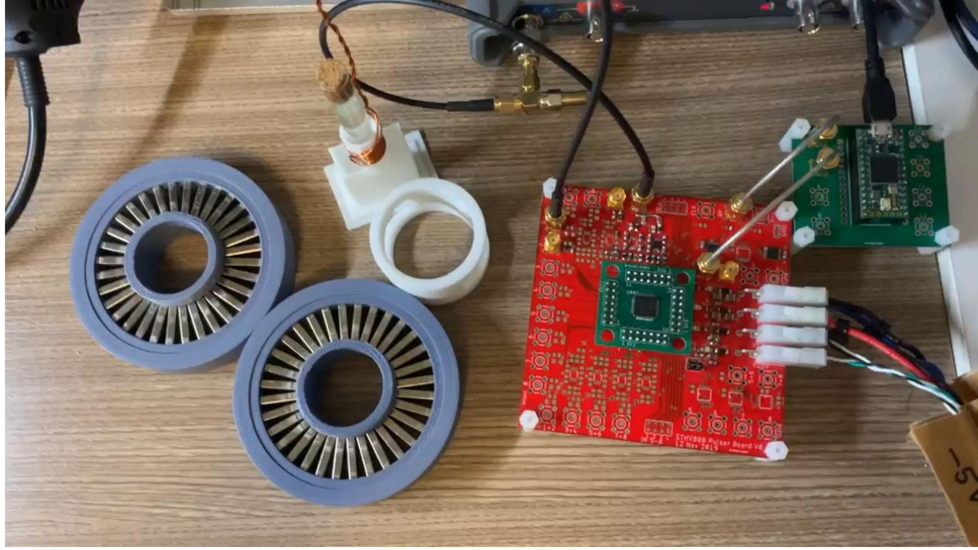

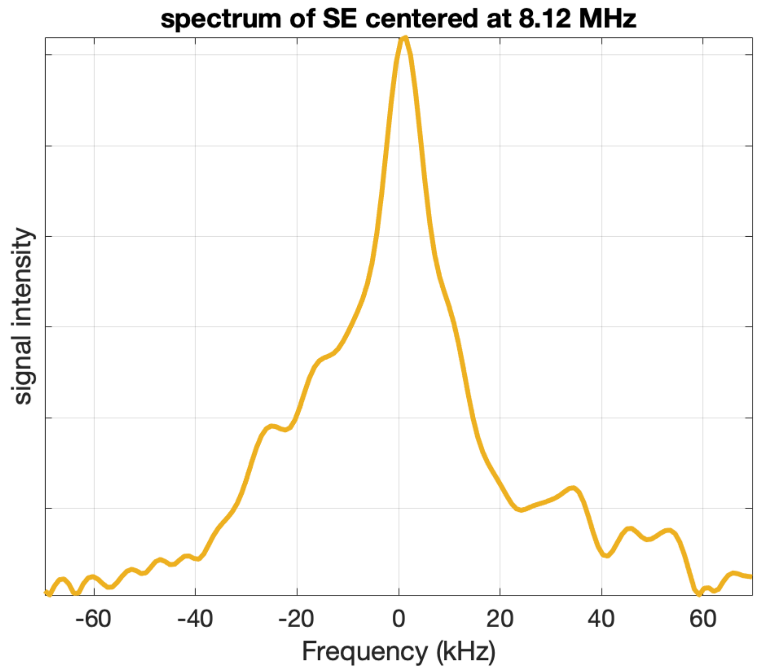

Field variation vs. magnet geometry (simulation)

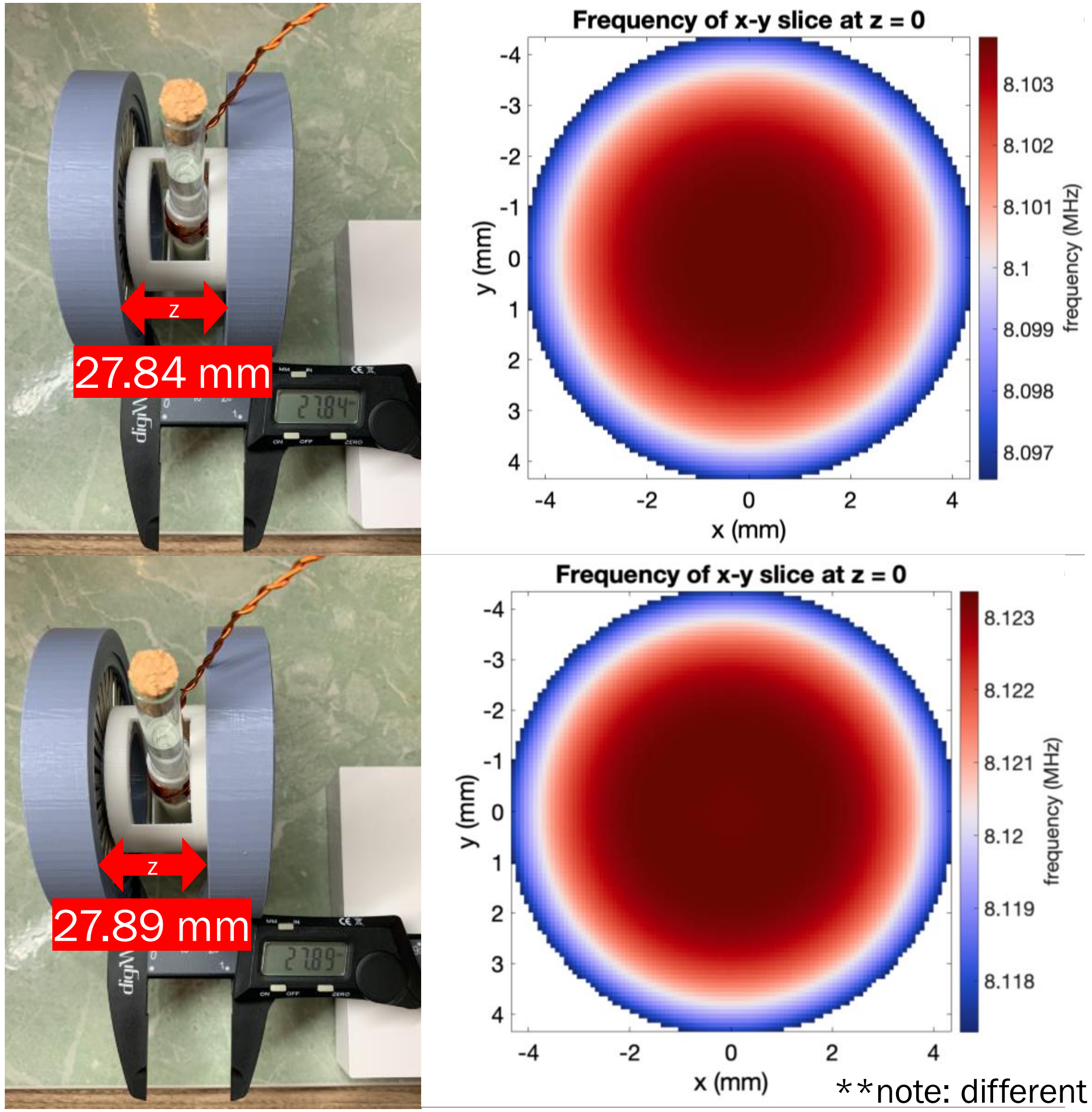

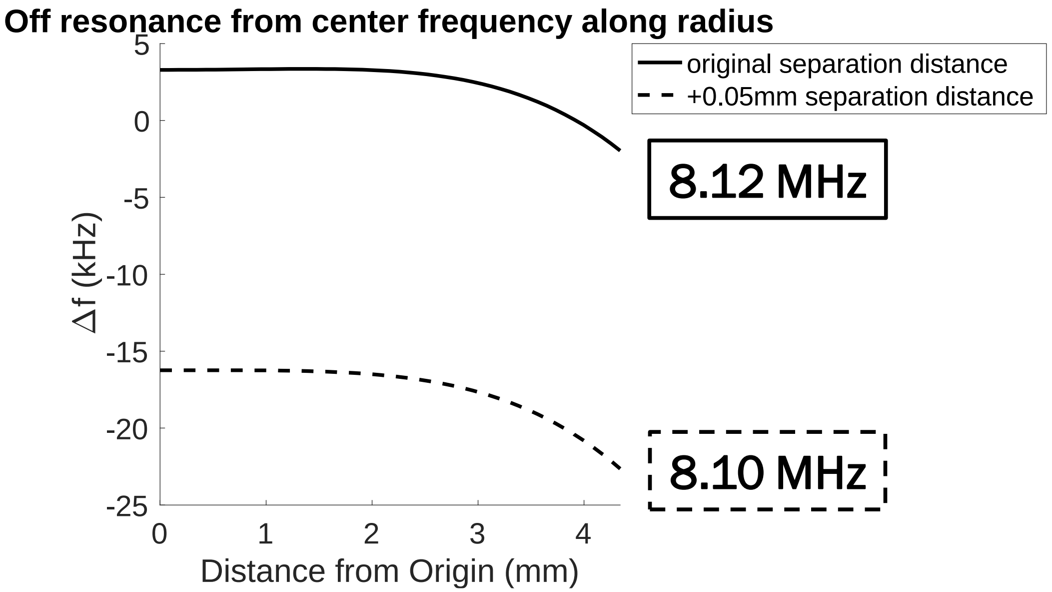

**note: different colorbar scales

Field variation vs. magnet geometry (measurement)

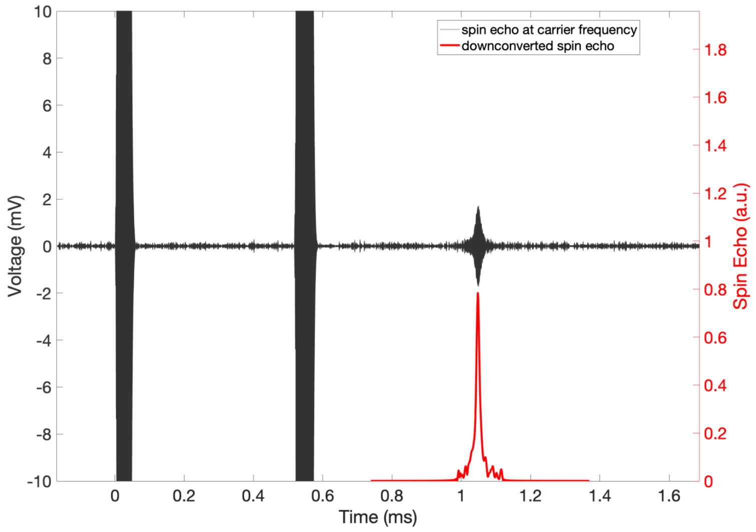

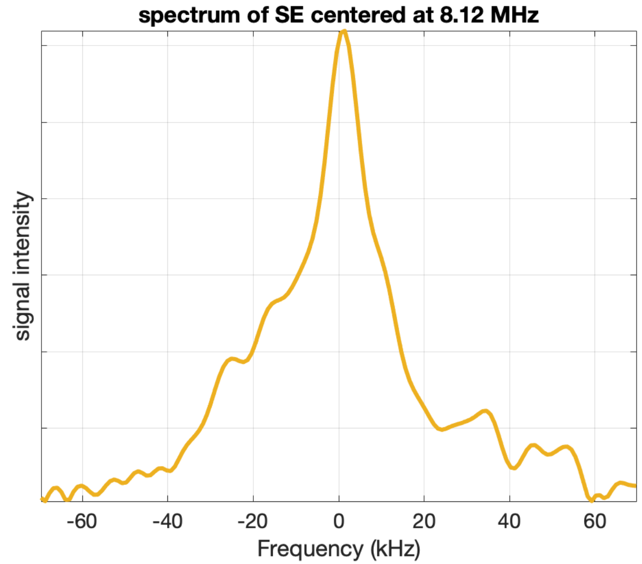

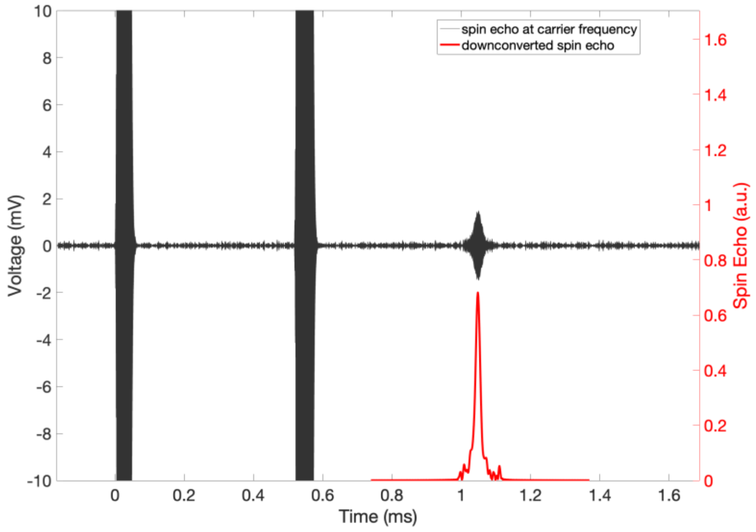

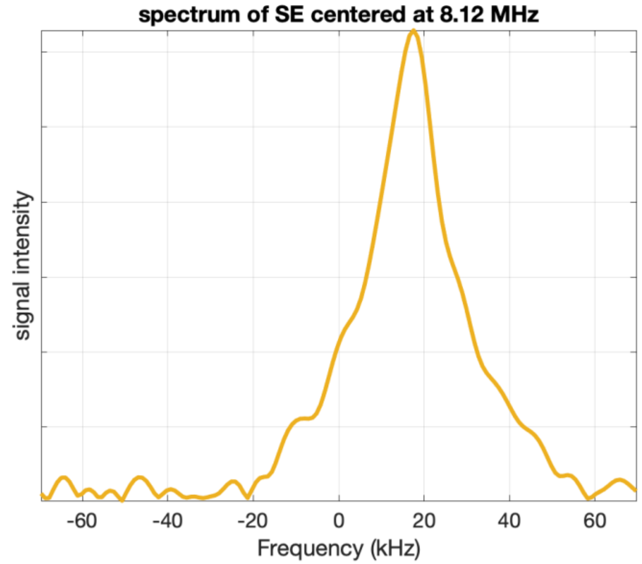

Using the **same 90° and 180°** pulse on 3 magnets with different center frequencies and homogeneity

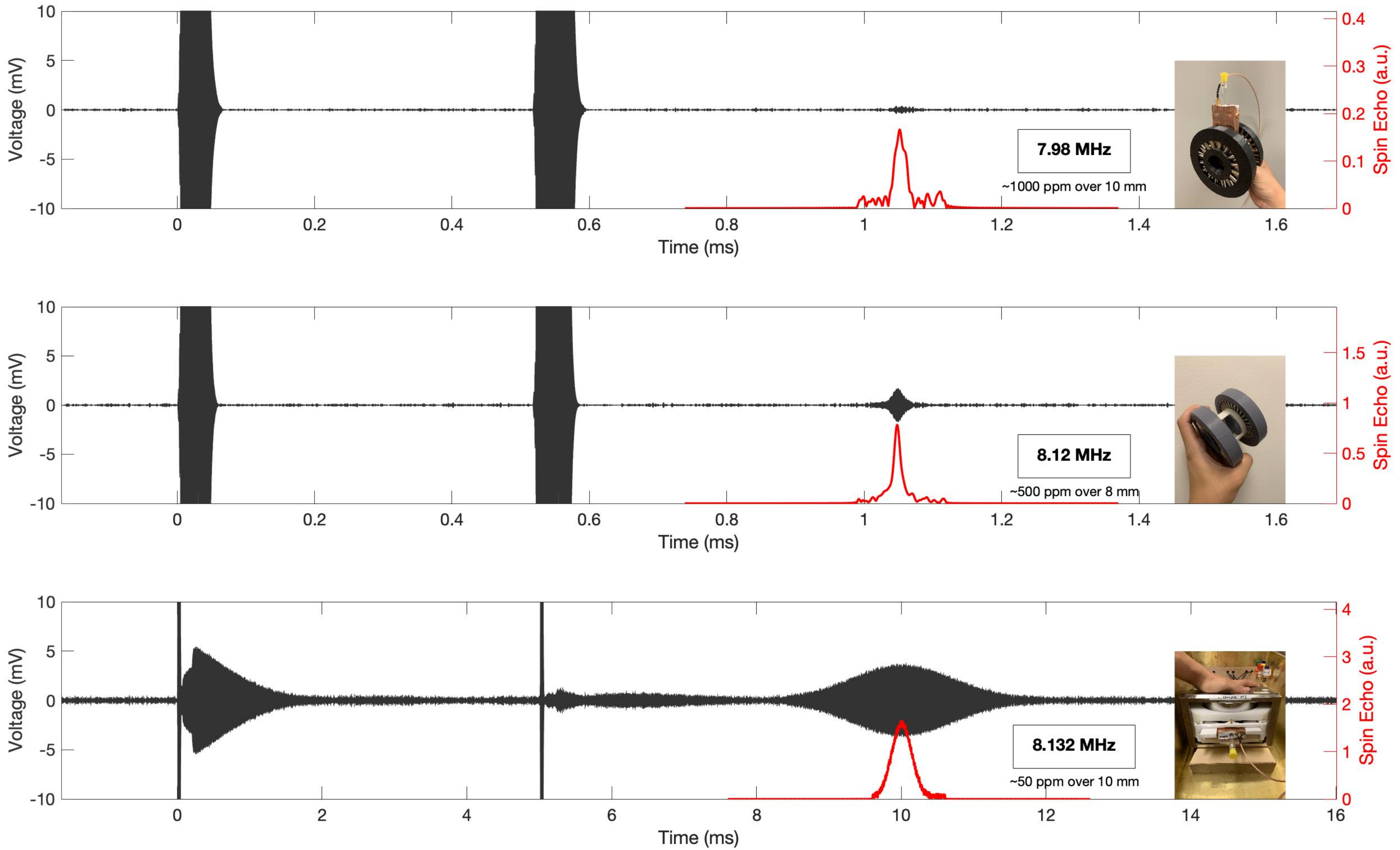

[3] Cooley et al., *Implementation of low-cost, instructional tabletop MRI scanners*. Int. Soc. Magn. Res. Med., 2014.

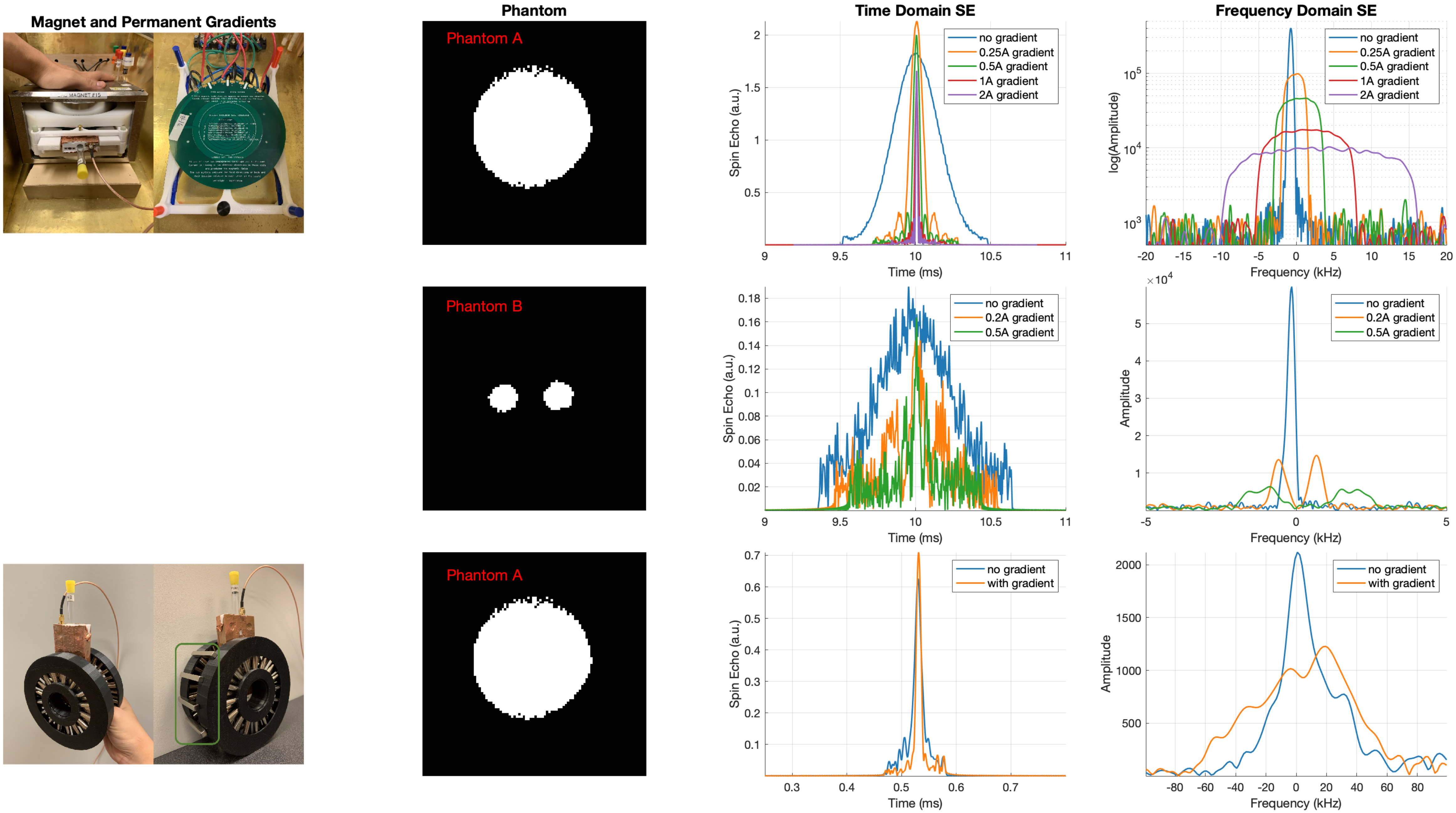

Magnet and Permanent Gradients
Phantom
Time Domain SE
Frequency Domain SE
Phantom A
Phantom B
Phantom A
no gradient
0.25A gradient
0.5A gradient
1A gradient
2A gradient
0.2A gradient
with gradient
Spin Echo (a.u.)
Time (ms)
log(Amplitude)
Amplitude
Frequency (kHz)

Acknowledgements

- NIH NIBIB R01EB018976
- MIT-MGH seed grant
- Skolkovo Institute of Science and Technology Next Generation Program
- MIT EECS department

Nick Arango
MIT

Jason Stockmann
Martinos/HMS

Elfar Adalsteinsson
MIT

Jacob White
MIT

Massachusetts Institute of Technology

MGH/HST Athinoula A. Martinos Center for Biomedical Imaging

MASSACHUSETTS GENERAL HOSPITAL

Harvard-MIT Health Sciences & Technology

HARVARD MEDICAL SCHOOL

Thank You!

Live Q&A Session
Engineering & Safety of MRI
Thursday, 13 August 2020
14:20 – 15:05 UTC